Garnet of the South Mountain Batholith, Nova Scotia

Sarah Catherine Hale

Submitted to the Department of Geology
of Smith College in partial fulfillment
of the requirements for the degree of
Bachelor of Arts with Honors

John B. Brady, Faculty Advisor

May, 2007

Table of Contents

ABSTRACT OF THESIS

GARNET OF THE SOUTH MOUNTAIN BATHOLITH, NOVA SCOTIA

The Devonian South Mountain Batholith (SMB) in southwestern Nova Scotia is the largest granitoid batholith of the Appalachian orogeny (MacDonald, 2001). The peraluminous granites of the SMB were emplaced above Avolonian rocks within the upper crust of Meguma Terrane in the Late Devonian (Benn, 1999). The SMB is believed to be a partial melt of the aluminous sedimentary rocks in the underlying Avolonian Basement (MacDonald, 2001). Garnet is a common mineral in the granodiorites, monzogranites and leucomonzogranites of the SMB (Allan and Clarke, 1981). Through the characterization of SMB garnets, this study considers how the granite melt interacted with country rocks.

Garnet crystals in the marginal units of the Halifax and Boot Lake Plutons in the South Mountain Batholith, Nova Scotia were found to be xenocrystic in origin. Garnet is abundant at contact zones between SMB granites and Meguma Group Country rocks and less abundant away from the contacts. Garnet also is found in close association with Meguma Group xenoliths. Most of garnets observed occurred in the center of biotite “clots”. Small anhedhral garnets (< 2mm) are commonly found in clots ~2 cm diameter. The anhedral shape of the garnets suggests that they have interacted with the magma and possibly dissolved.

SEM/EDS analyses show that SMB garnets are almandine-rich, with compositions similar to those observed for garnet in the surrounding Meguma metamorphic rocks. Garnets from the Boot Lake and Halifax Plutons all have spessartine-enriched rims. The Mn rims around the garnets are evidence of a chemical interaction between xenocrystic garnets and a granite magma. The Mn may have diffused into the xenocrystic garnet from the

peraluminous granite, as the garnet equilibrated with the magma. Another possibility is that the source of the Mn was not the magma, but the garnet itself; the Mn may have preferentially stayed behind and diffused into the remaining garnet as the crystal partially melted.

Experiments were performed to investigate the origin of the Mn rims observed for garnets in the Peggy's Cove monzogranite. Polished slices of a Meguma garnet crystal were surrounded by crushed glass, made by melting a SMB granite sample, and heated with excess water at 5 kb in a piston-cylinder press. In a sample heated at 800°C, the garnet crystal grew a rim that was enriched in Mg. In a sample heated at 700°C, the garnet crystal clearly reacted with the melt, consuming garnet to produce biotite. These results provide further evidence for a xenocrystic origin for the garnets surrounded by biotite and suggest that the xenocrysts were entrained at temperatures between 700° and 800°C.

Sarah Catherine Hale
Smith College Department of Geology
Northampton, Massachusetts
May, 2007

Acknowledgements

I would first like to thank my adviser John Brady who has always challenged me, sparked my curiosity, and encouraged me to think harder and ask questions. This project would not have been possible without his support, enthusiasm, and patience.

Special thanks to Jade Star Lackey for leading a top-notch field project and also thanks to all of the Keck Nova Scotia crew for a wonderful time last summer!

I feel incredibly lucky to have been a part of the Smith College Geology community for the past four years. Thanks to Bob Newton, Mark Brandriss, Al Curran, Steve Gaurin, John Brady, Amy Rhodes, Bob Burger, and Bosiljka Glumac for being so dedicated to their students. Thanks to Tony Caldanaro for helping me with my sample preparation, computer troubles, and for being a great cheerleader. Thanks to Kathy Richardson and Ann Pufall for being so helpful and friendly. Also- thanks to all of my fellow Smithie geologists for their delightful camaraderie and support and especially to my partner in crime, Jezra Beaulieu for her humor and company.

I would like to thank my roommate and dear friend, Arminé Thompson, for keeping me company in the lab, late-night coffee runs, and countless other kind favors.

Thanks to all of my family for their support. I would especially like to thank my aunt, Alison Rieser, who has always encouraged me to pursue science and has been a mentor and an incredible role model for me.

Thanks to the William M. Keck Foundation and the Nancy Kershaw Memorial Fund for financial support.

List of Figures

List of Tables

CHAPTER 1: REGIONAL GEOLOGY AND BACKGROUND

THE SOUTH MOUNTAIN BATHOLITH

The Province of Nova Scotia marks the northeastern most part of the Appalachian region. It was formed by the accretion of different landmasses along the northeast margin of the ancient North American continent (MacDonald, 2001). Meguma and Avalon terranes form two distinct halves of Nova Scotia; they are separated by the Cobequid Chedabucto Fault System (Fig. 1). It has previously been suggested that the metasedimentary rocks of the Meguma Terrane docked with a Laurentian landmass that had previously been accreted Avalonian terrane during the Devonian Acadian Orogeny (Keppie, 1993; Benn, 1999). A recent study by proposes that there is paleogeographic evidence for a different tectonic history. Murphy and Keppie (2005) suggest that Avalonia and Meguma Terranes docked onto Laurentia by the Early Silurian and that the accretion of these three landmasses coincided with the closing of the Iapetus Ocean.

The Devonian Granites of the South Mountain Batholith (SMB) in southwestern Nova Scotia make up the largest (7300 km^2) granitoid batholith of the Appalachian orogen (MacDonald, 2001) (Fig. 1). The SMB is an example of a peraluminous (aluminum-enriched, where A/CNK >1) granite batholith emplaced within an active orogen (Clarke et al., 2004; Benn, 1999). The SMB is believed to be a partial melt of the aluminous sedimentary rocks in the underlying Avalonian Basement (MacDonald, 2001). The formation, extraction, transport and emplacement of immense amounts of peraluminous granite magma within the meta-sediments of the Meguma Terrane occurred over a few million years (Benn, 1999).

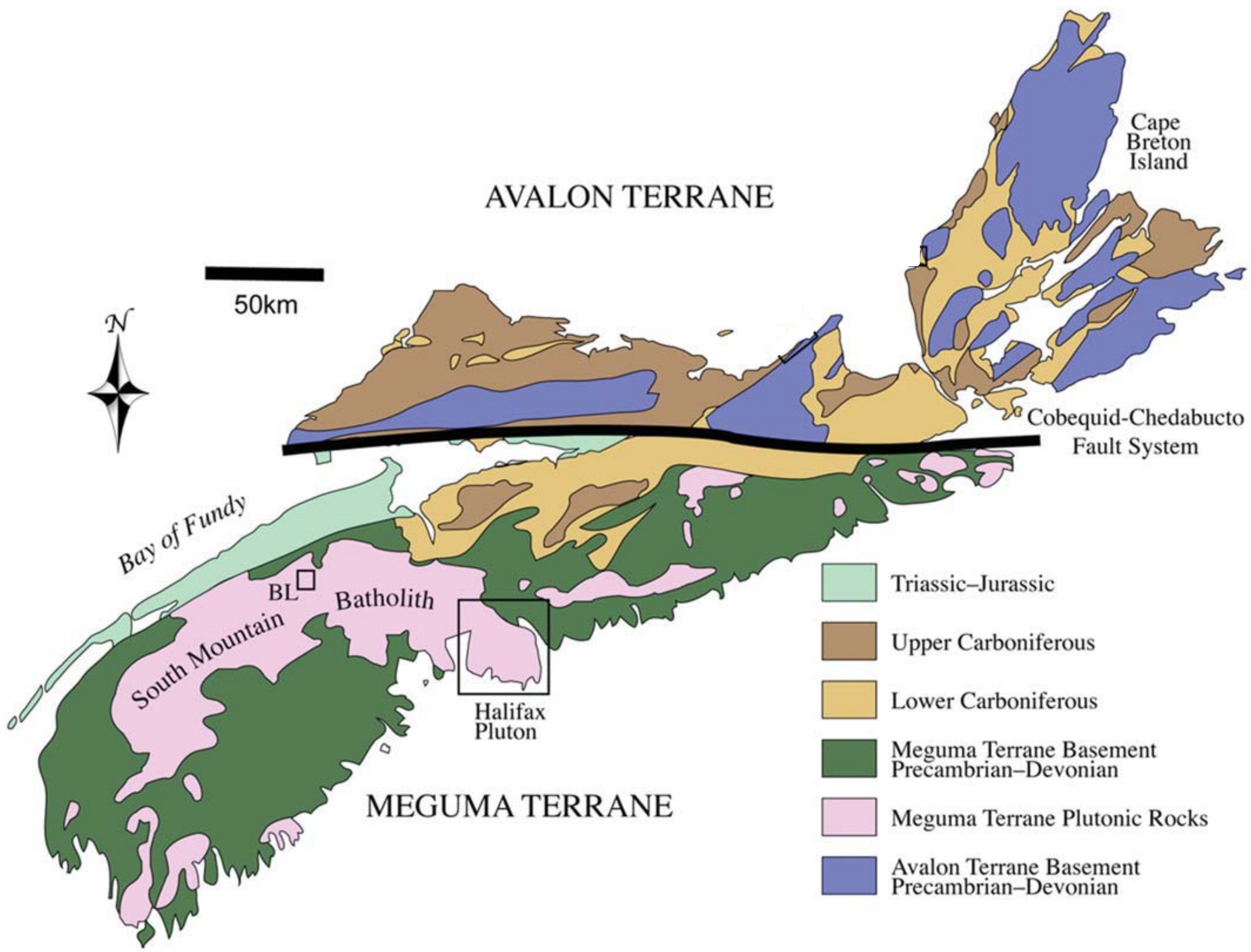

Figure 1: Geology of Nova Scotia. The two plutons studied in this paper, the Boot Lake (BL) and Halifax Plutons are shown in the boxed area. Modified from Davis and Browne, 1997.

The Meguma Terrane is made up of the Cambro-Ordivician turbidites of the Meguma Supergroup that were deposited on the northwestern continental margin of Africa (Benn, 1999). The structural basement of the Meguma Terrane is thought to correspond to the sillimanite-grade gneisses and schists of the Liscomb Complex that are exposed in an area just south of the Cobequid-Chedabucto fault zone (Benn, 1999). The significance of the contamination of SMB granites by Meguma Group country rocks is uncertain because of discrepancies between field observations and whole-rock isotopic analysis; while field data suggest a higher degree of contamination for the marginal units of the SMB, whole-rock, Sr-Nd isotopic data suggest an upper limit of ~33% of contamination for the central, most evolved rocks (leucogranites) of the SMB (Erdmann, 2007).

LITHOLOGIES

The SMB has been subdivided and mapped into 13 plutons based on field relationships and compositional similarities. Five plutons are designated as early, Stage I plutons, consisting of biotite granodiorite and biotite monzogranite with minor fine-grained leucomonzogranite (MacDonald, 2001). These were the first plutons to be emplaced. The Stage I plutons were intruded by eight Stage II plutons, which consist of muscovite-biotite monzogranite, coarse- and fine-grained leucomonzogranite and muscovite leucogranite with minor biotite granodiorite and biotite monzogranite (MacDonald, 2001). The Boot Lake (Stage I) and The Halifax (Stage II) Plutons are the focus of this study (Fig. 1).

Previous petrographic studies show that the six main rock types of the 13 plutons have similar mineralogical characteristics (MacDonald, 2001). While most of the rock-forming mineral phases in the granites are of magmatic origin, many minerals also formed by xenocrystic and metasomatic processes (MacDonald, 2001). One mineral of such occurrences is garnet.

Boot Lake Pluton

The Boot Lake Pluton is a small (~ 4km) discrete body of granodiorite surrounded by two stage I plutons: The Scrag Lake Pluton and the Cloud Lake Plutons. It hosts several metasedimentary bodies of the Halifax Formation (Meguma Group) and contains an abundance of millimeter to meter-scale xenoliths.

Halifax Pluton

The Halifax Pluton is the largest stage II pluton of the SMB and also the most extensively studied (MacDonald, 2001). The pluton is sub-circular in shape and contains four main zoned map units: biotite granodiorite, megacrystic biotite monzogranite, coarse grained leucomonzogranite and muscovite-biotite monzogranite (Figure 2). The Sandy Lake and Peggy's Cove monzogranites at the northern and southern edges of the pluton encircle the Harrietsfield muscovite-biotite monzogranite and the Halifax Peninsula coarse-grained monzogranite. A thin (< 1-3 km wide) biotite ganodiorite unit is mapped along the northeast margin of the pluton in sharp contact with the meta-sedimentary rocks of the Meguma Group.

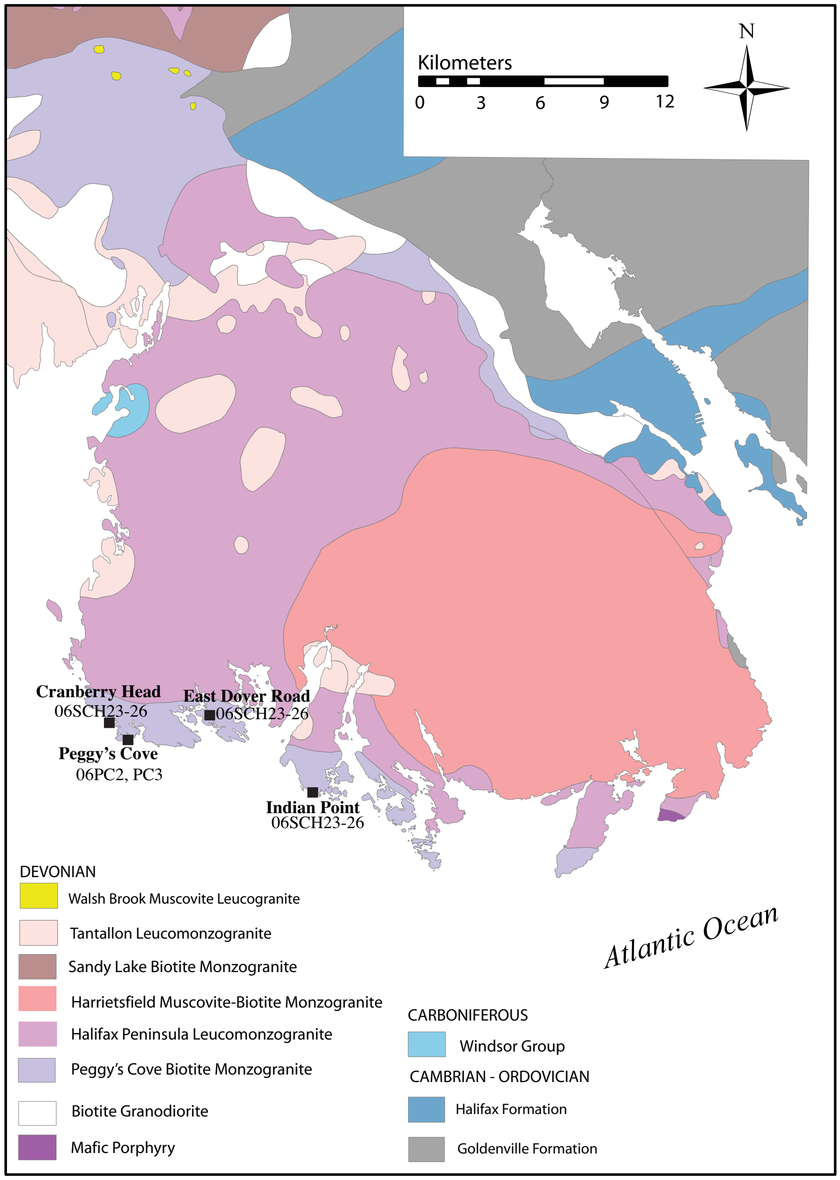

Figure 2: Map of lithologies in and around the Halifax Pluton, with sample locations at Cranberry Head, Peggy's Cove, East Dover Road, and Indian Head indicated by black boxes. (Modified from MacDonald et al., 2001)

GARNET

Garnet is an uncommon mineral in igneous rocks. Its most common occurrences in igneous rocks are in pegmatites, aplite dikes, and in peraluminous granites (Leake, 1967; Green, 1977; Allan and Clarke, 1981; Miller and Stoddard, 1981; Deer et al., 1982). du Bray (1988) notes that "correlations between garnet composition, host granitoid composition and tectonic setting suggest that garnet chemistry can be employed as an indicator of the tectonic regime prevailing a the time of host granitoid genesis." Garnet is present throughout the SMB in trace amounts in many rock units and is very common in the marginal units of the Boot Lake and Halifax Plutons. It occurs on both sides of and in proximity to the contact between the peraluminous granites of the SMB and the metamorphic rocks of the Meguma Group.

Allan and Clarke (1981) conducted a study of garnet in the South Mountain Batholith and define three types of garnet based on textural and chemical characteristics. They suggest that garnets in the SMB have both xenocrystic and magmatic origins (Allan and Clarke, 1981). Metasomatic processes have also been used to explain the presence of garnet in SMB granites (Kontak, 1988). The focus of this study is to characterize the garnets found in the marginal units of the Halifax and Boot Lake Plutons.

CHAPTER 2: PURPOSE AND METHODS

GOALS

Through the characterization of garnets, this study considers how the South Mountain Batholith (SMB) granite magma interacted with country rocks. This was accomplished by collecting garnet-bearing samples in various rock bodies of the batholith. Garnets that appeared to be of both magmatic and xenocrystic origin were considered. Although the original goal was to collect both magmatic and xenocrystic garnets, garnets that appear to be of a xenocrystic origin were more abundant and were sampled more extensively.

METHODS OF STUDY

Fieldwork in the southern mainland of Nova Scotia was conducted during the summer of 2006. Samples collected in the Boot Lake and Halifax Plutons were selected on the basis of their garnet content. Garnet was found and collected in the granodiorites and monzogranites of the SMB, as well as in the meta-sedimentary rocks of the Meguma Group. A few hand samples that didn't contain garnet were also collected to investigate the lithologies of the batholith. A latitude and longitude were recorded with a GPS unit at each sample location. Thin sections were made of some samples. Epoxy mounts were prepared of other garnet samples that were too small or friable to be made into thin sections. Lab work consisted of petrographic analysis of thin sections and analysis of garnet compositions in the epoxy mounts and some thin sections by scanning-electron microscopy with energy dispersive x-ray spectrometry (SEM/EDS).

STUDY AREA AND SAMPLE LOCATIONS

Samples were collected from three plutons in the Batholith, as well as the Meguma Group metasedimentary rocks that host the granites. Most samples came from the Boot Lake (stage I) and the Halifax (stage II) plutons. Only a few samples came from the Scrag Lake (stage I) pluton. Most of the garnet-bearing samples collected were small (~ 2 cm in diameter) biotite clots. (See Fig. 2 and Table 1 for sample locations)

Sample	Latitude Min	Deg	Sec	Longitude Min	Deg	Sec	Geographic Location	Unit	Sample Type
06SCH1	44	50	40	63	48	18	101 northbound	Goldenville Formation	hand
06SCH2	44	53	31	63	52	57	101 northbound	Halifax Formation (COH)	hand
06SCH3	44	53	31	63	52	57	101 northbound	COH	hand
06SCH4	44	53	31	63	52	57	101 northbound	COH	hand
06SCH5	44	43	58	63	48	29	213	Biotite Granodiorite (gd), Halifax Pluton	hand
06SCH6	44	39	28	63	40	30	Halifax	COH	hand
06SCH7	44	39	28	63	40	30	Halifax	COH, (gd)	hand
06SCH8	44	30	46	63	51	47	East Dover Rd.	Peggy's Cove Biotite Monzogranite (PCmg)	hand
06SCH9	44	31	57	64	7	13	Upper Blanchford Road	Sandy Lake Biotite Monzogranite	hand
06SCH10	44	31	23	64	7	15	Upper Blanchford Road	COH	hand
06SCH11	44	51	55	64	46	33	Scrag Lake	Scrag Lake Biotite Monzogranite	hand
06SCH12	44	52	9.7	64	49	24	Boot Lake	Boot Lake Granodiorite (DCgdBL)	hand
06SCH13	44	52	9.7	64	49	24	Boot Lake	DCgdBL	epoxy
06SCH14	44	52	9.7	64	49	24	Boot Lake	DCgdBL	epoxy
06SCH15	44	52	9.7	64	49	24	Boot Lake	DCgdBL	epoxy
06SCH16	44	52	9.7	64	49	24	Boot Lake	DCgdBL	epoxy
06SCH17	44	52	9.7	64	49	24	Boot Lake	DCgdBL	epoxy
06SCH18	44	52	9.7	64	49	24	Boot Lake	DCgdBL	hand
06SCH20	44	28	10	63	47	43	Indian Point	PCmg	epoxy
06SCH21	44	28	8.8	63	47	42	Indian Point	PCmg	epoxy
06SCH22	44	51	58	63	49	40	Indian Point	PCmg	epoxy
06SCH23	44	29	59	63	55	29	Cranberry Head	PCmg	epoxy
06SCH24	44	29	59	63	55	29	Cranberry Head	PCmg	hand
06SCH25	44	29	59	63	55	29	Cranberry Head	PCmg	epoxy
06SCH26	44	29	59	63	55	29	Cranberry Head	PCmg	epoxy
06PC2	44	29	32	63	54	43	Peggy's Cove	PCmg	epoxy
06PC3	44	29	32	63	54	43	Peggy's Cove	PCmg	epoxy
06SMB9	44	28	12	63	47	52	Indian Point	PCmg	epoxy
SMB10	44	28	11	63	47	53	Indian Point	PCmg	hand
SMB15	44	51	58	64	49	40	Boot Lake	COH	hand

Table 1: Sample locations and rock types.

CHAPTER 3: FIELD OBSERVATIONS

HALIFAX PLUTON

Samples were collected from three main units around the margin of the Halifax Pluton. Most of the sampling was conducted in the Peggy's Cove monzogranite because of its accessibility and garnet content. Sampling was also conducted in the Sandy Lake unit, as well as in the granodiorite in mixing and northern contact zones between the Halifax Pluton and the meta-sedimentary rocks of the Meguma Group.

Peggy's Cove Monzogranite

The Peggy's Cove Monzogranite is a 1-3km wide unit that outcrops along the Atlantic Coast and forms the southern rim of the Halifax Pluton. The unit displays textural diversity that varies regionally. The biotite-monzogranite contains abundant xenoliths and enclaves that vary in size and composition. Megacrystic zones, and pegmatitic features occur in dikes that cross-cut the unit as well as in "balls" and "swirls." Garnet occurs throughout the unit in cm-scale clots of biotite. In some locations, small euhedral garnets occur without clots of bioite, and are interpreted to be magmatic garnet in origin (MacDonald, 2001).

Peggy's Cove

Peggy's Cove is the type locality of the Peggy's Cove biotite monzogranite, the southern outer-most unit of the pluton. It outcrops prominently on the western mouth of St. Margaret's Bay. Thick (> 1m) aplite and pegmatite dikes transect the unit and were studied intensively by Kontak (2002). Garnet-bearing xenoliths are common in this locality. They occur in circular (1-2cm) clots of biotite and in close proximity to the aplite and pegmatite dikes (Figure 3). Biotite schlieren were observed but were not as

Figure 3: Photograph of a small garnet-rich biotite clot in the Peggy’s Cove biotite monzogranite at Peggy’s Cove. Quarter for scale.

Figure 4: Photograph of a decimeter scale intermediate enclave with two garnet-bearing biotite clots in the Peggy’s Cove biotite monzogranite at Indian Point. Hammer for scale.

abundant as in other locations. The garnet-bearing biotite clots collected at Peggy's Cove were too small and friable to be made into thin sections. Two clots (~1.5 cm) filled with small (~1mm) garnets concentrated in their core were made into epoxy mounts to be analyzed by SEM/EDS.

Indian Point

This coastal exposure of the Peggy's Cove monzogranite is located near the Village of Prospect on the southwestern mouth of Prospect Bay. While no felsic dikes were observed at Indian Point, large (~1m) circular to ellipsoidal enclaves, rimmed by feldspar megacrysts (cm-scale crystals) with pegmatitic textures were observed. Smaller enclaves (decimeter scale) of intermediate to mafic composition were also observed (Figure 4). Circular garnet-bearing xenoliths with biotite and feldspar rims are also present. Two garnet-biotite clots were made into epoxy mounts to be analyzed by SEM/EDS (SMB-10, SCH-22).

Cranberry Head

Cranberry Head is a small point northwest of Peggy's Cove. The monzogranite at this location is texturally unique. It is rich in meter-scale swirling biotite-schlieren and intermediate to mafic enclaves with rims of megacrystic feldspars. Garnet at Cranberry Head is abundant in biotite clots similar to those observed in other localities, but also occurs in more felsic-rich clusters (Figure 5). Garnet-bearing xenoliths and enclaves are varied in size and texture at this location. While some occur in the circular ~1-2 cm clots of biotite clots, others occur in larger (2-6cm) clots of biotite and feldspar. Larger, more felsic clots tend to be more elliptical in shape and are found in the rims of several "intermediate enclaves."

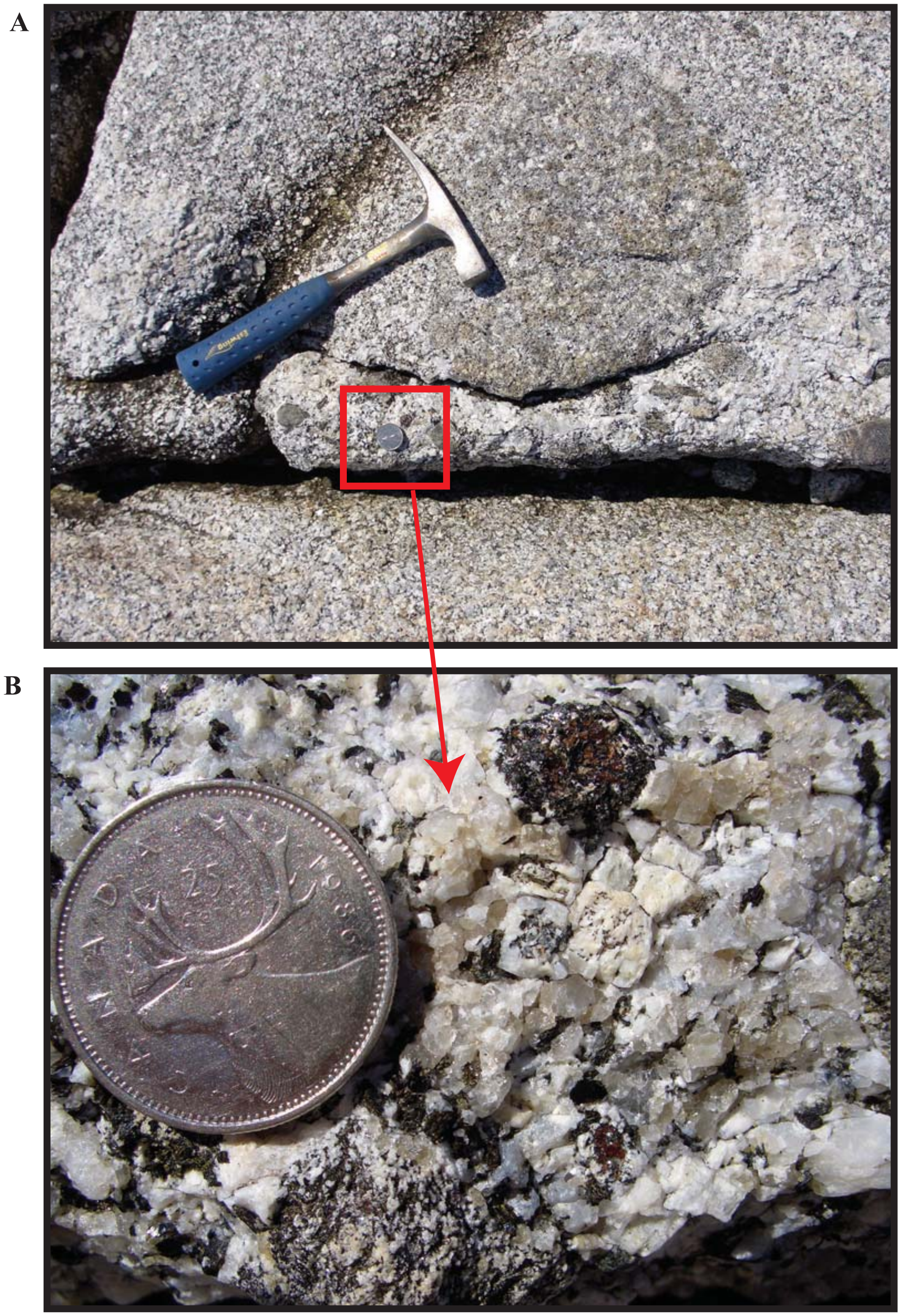

Figure 5: (A) Photograph of an intermediate enclave with a megacrystic rim in Peggy's Cove biotite monzogranite at Cranberry Head. Hammer for scale. (B) A garnet rich biotite clot in the megacrystic rim of the enclave shown in A, containing more feldspar and quartz then garnet-rich biotite clots observed in other locations.

East Dover Road

This location is a roadside outcrop of the Peggy's Cove biotite monzogranite. The unit at this location is slightly more felsic and less biotite-rich. Large (~4cm) feldspar megacrysts are prevalent and are commonly twinned. A small (<3mm) euhedral garnet was observed and lacked a textural association with biotite (Figure 6). A large (10 kg) sample collected to see if magmatic garnets were present in this roadside outcrop of Peggy's Cove monzogranite.

Sandy Lake Monzogranite

The Sandy Lake biotite monzogranite forms the northern rim of the Halifax Pluton. Unaligned alkali feldspar megacrysts were prevalent.

Deep Cove

A roadside outcrop of the Sandy Lake biotite Monzogranite was observed on ~500 m northeast of a contact with the Halifax Formation. The exposure was poorly lit and covered with vegetation. A hand sample containing a xenolith and a garnet-biotite clot was collected from this location (Figure 7).

Figure 6. Photograph of an isolated euhedral garnet crystal in Peggy's Cove biotite monzogranite at East Dover Road. Coin for scale.

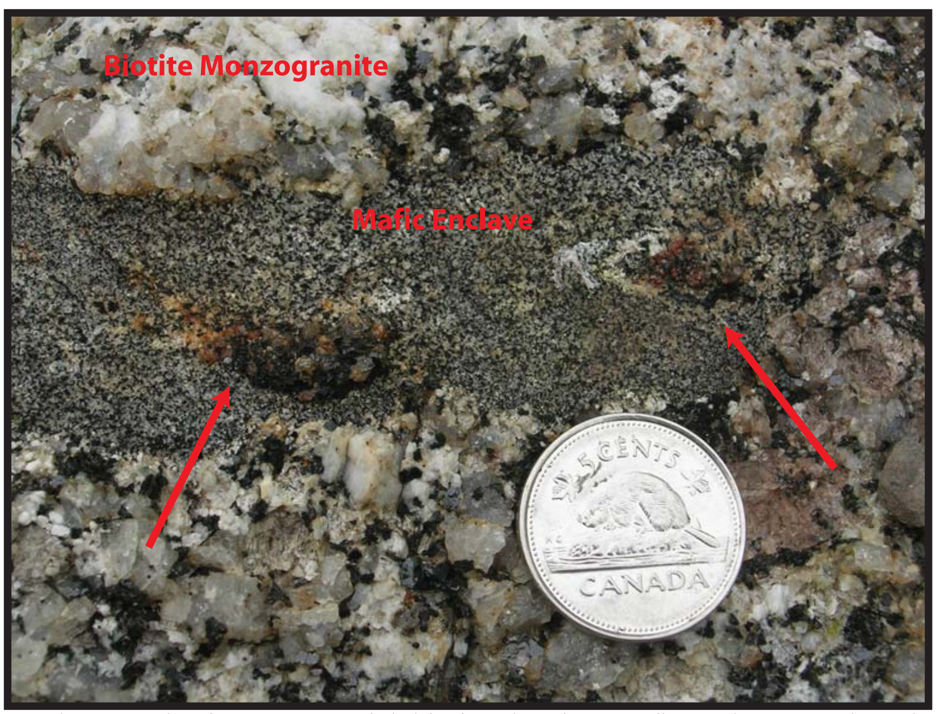

Figure 7. Photograph of two garnet-rich biotite clots in a mafic enclave. Sandy Lake biotite monzogranite near Deep Cove. Coin for scale.

Contact Granodiorite

Samples from the biotite-granodiorite unit on the margin of the Halifax Pluton were collected at several locations in the Halifax-metro area. Contact relationships between the Halifax Pluton and the Meguma Group are structurally and texturally complex. Pegmatitic dikes containing large alkali feldspar megacrysts occur in unaligned clusters. Garnet-rich layers are present at the contact between the biotite granodiorite and the Halifax Formation (Figure 8). While garnet occurs in close proximity to biotite, well-developed biotite clots were not observed.

BOOT LAKE PLUTON

Boot Lake Granodiorite

The Boot Lake unit is a highly contaminated discrete body of granodiorite with complex mixing textures. The unit is rich in biotite, muscovite, megacrystic feldspars and xenoliths that range in size from ~5-30 cm. Samples were collected from a single outcrop that was more abundant in garnet and garnet-bearing xenoliths than in any other location considered in this study (Figure 9). Garnet occurs in meta-sedimentary xenoliths, contacts between xenoliths and granodiorite, and in the matrix of the granodiorite.

Metasedimenary xenoliths are inferred to be from the Meguma Group country rocks and display alternating layers psammite and garnet-bearing pelite (Figure 10). Several garnet-biotite “clots” appear to trail out of the meta-sedimentary xenoliths into the granodiorite (Figure 9). While some garnets occurred in biotite clots, others were found to occur in close association with feldspar (Figure 11).

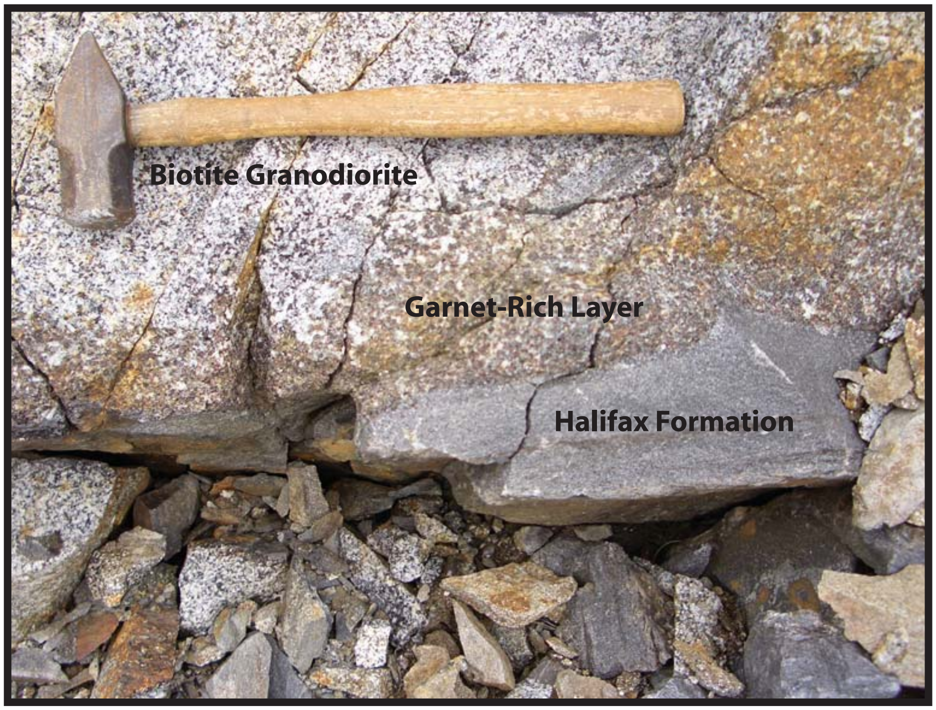

Figure 8: Photograph of a garnet-rich layer at a contact between the Halifax Formation and the biotite granodiorite along the margin of the Halifax Pluton. Rock hammer for scale.

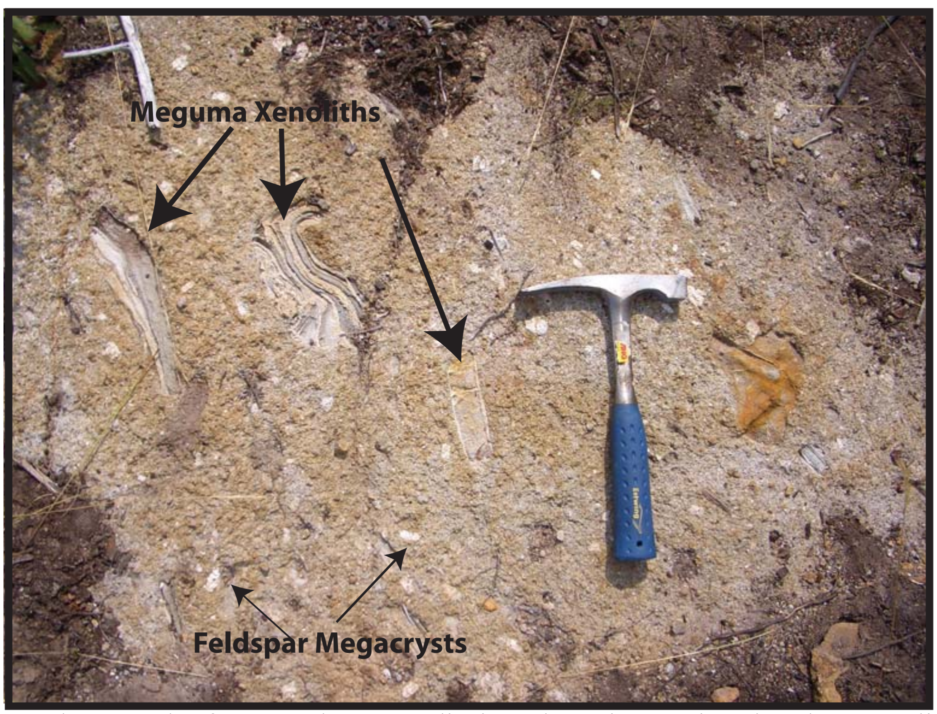

Figure 9: Photograph of Boot Lake Granodiorite. The unit contains abundant xenoliths, garnet, and feldspar megacrysts. Rock hammer for scale.

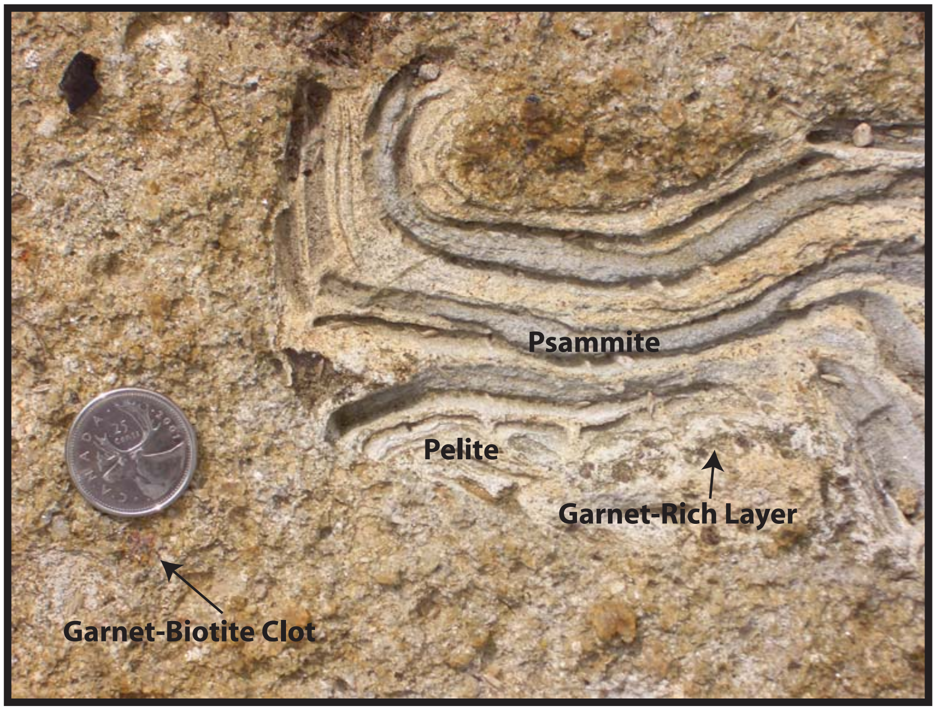

Figure 10: Photograph of Meguma Group xenolith with alternating layers psammite and garnet-bearing pelite at Boot Lake. Some garnet appears to be trailing from the xenolith into the granodiorite. Coin for scale.

Figure 11: Photograph of garnets at Boot Lake that have feldspar reaction rims and lacks a textural association with biotite (arrows point toward garnets). Coin for scale.

SCRAG LAKE PLUTON

The Scrag lake pluton is the largest (2460 km^2) stage 1 pluton of the SMB. It is elliptical in shape and takes up much of the northwestern area of the Batholith. The Scrag Lake biotite monzogranite is the most abundant rock type of the pluton.

Scrag Lake Monzogranite

One sample was collected from an outcrop of the Scrag Lake biotite monzogranite on an abandoned logging road. Megacrystic feldspars were abundant. Small garnets were thought to be present in the sample though it was hard to tell because of the highly weathered nature of the sample.

CHAPTER 4: PETROGRAPHY

PURPOSE

The purpose of petrography in this study is to characterize and provide a petrologic context for the garnets of the South Mountain Batholith (SMB). Petrographic analyses were conducted on fourteen thin sections from hand samples collected in and around the margins of the SMB. Ten of these samples came from granites in three separate plutons of the SMB. Because this study also considers the interaction between granite bodies and country rocks, it was also important to characterize country rocks. Four thin sections were prepared from two different Meguma Group units: the Halifax Formation and the Goldenville Formation.

HALIFAX PLUTON

Peggy's Cove Monzogranite

Petrographic analyses were conducted on two thin sections from The Peggy's Cove Monzogranite (SCH-8, and SCH-24 were studied). The unit contains the same modal percentages in both sections; the biotite monzogranite consistently has equal amounts of quartz, plagioclase and alkali feldspar with 10-17% biotite. There is some variability in alkali feldpars within the unit; both orthoclase and perthite were observed. Feldspars have been partially to completely altered to sericite and some of the biotite displays chloritization. Thin sections also contain minor amounts of muscovite (~1%) and trace amounts of illmenite, monazite, and zircon. Garnet was present in one thin section (SCH-24). While the texture of the unit is variably megacrystic and contains cm-scale feldspars, intermediate enclaves and xenoliths are more equigranular and contain mm-scale crystals.

Halifax Pluton	Mineralogy	Garnet Occurrence & Notes
06SCH-8	quartz, perthite, plagioclase, biotite, muscovite, flourite	no garnet observed, chloritization of biotite, seritization of feldspars
06SCH-24	quartz, orthoclase, plagioclase, biotite, muscovite, garnet, illmenite	~1-2mm subhedral to anhedral garnets in biotite clot
06SCH-9	quartz, orthoclase, plagioclase, biotite, muscovite	no garnet observed
06SCH-3	quartz, orthoclase, plagioclase, biotite, muscovite, garnet	abundant euhedral-subhedral garnet ~1-2mm in diameter with quartz, illmenite & biotite inclusions
06SCH-4	quartz, orthoclase, plagioclase, biotite, muscovite, garnet	~1-2mm subhedral to anhedral garnets associated with biotite
05SCH-5	quartz, orthoclase, plagioclase, biotite, muscovite, garnet	~1-2mm subhedral to anhedral garnets associated with biotite
Boot Lake Pluton		
06SCH-12	quartz, orthoclase, plagioclase, biotite, muscovite, illmenite	no garnet observed
06SCH-17	quartz, orthoclase, plagioclase, biotite, muscovite, illmenite, garnet	≤1.5mm anhedral garnets in biotite clot
06SCH-18	quartz, orthoclase, plagioclase, biotite, muscovite, illmenite, garnet	~2-3mm subhedral-anhedral garnets
Scrag Lake Pluton		
06SCH-11	quartz, orthoclase, plagioclase, biotite, muscovite	no garnet observed, contains mafic fine-grained enclave
Meguma Group Country Rocks		
06SCH-1	quartz, orthoclase, plagioclase, clay minerals	quartz rich, no garnet observed, no distinct foliations or structures
06SCH-2	quartz, orthoclase, plagioclase, biotite, muscovite, illmenite	no garnet observed
06SCH-10	cordierite, andalusite, sillimanite, pyrite, graphite	no garnet observed, sillimanite replacing some andalusite crystals
06SMB-15	garnet-hornfels facies: biotite, muscovite, albite, quartz, zircon, garnet	larger euhedral garnets, lined with thin biotite and muscovite rim, quartz and illmeite inclusions

Table 2: Thin section mineralogy and garnet content of South Mountain Batholith Granites and Meguma Group country rocks.

Cranberry Head

One hand-sample (SCH-24) collected from the rim of a circular intermediate enclave at Cranberry Head was made into a thin section. It contains portions of a xenolith, intermediate enclave, and two biotite clots with garnet. The thin section made from this sample displays these textural variations. The garnets found in the biotite clot are ~1-2mm, subhedral to anhedral, and are surrounded by biotite with some muscovite and feldspar (Fig 12). Three epoxy mounts were prepared of biotite clots from this location (SCH-23, SCH-25, SCH-26). Two of them have similar textures to the clot analyzed in thin section; however, SCH-25 was found in an elliptical clot of biotite, quartz, and feldspar.

East Dover Road

The East Dover Road sample (SCH-8) contains cm-scale felspar megacrysts (Fig 13). The thin section of this sample contains plagioclase, perthitic alkali feldspar, and possibly small amounts of microline. Some of the felspars have been altered to sericite. and some of the biotite displays chloritization. Garnet was not present in the thin section. Trace amounts (< 1%) of fluorite were observed.

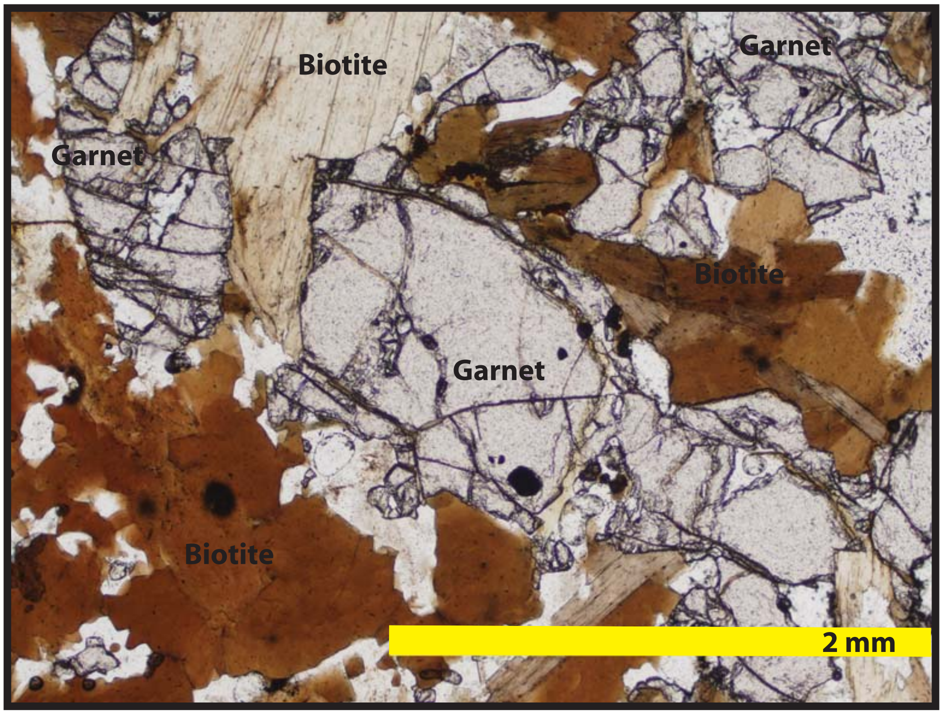

Figure 12: Photomicrograph of biotite clot with anhedral garnets in Peggy's Cove Biotite Monzogranite at Cranberry Head (SCH-24) Plane light.

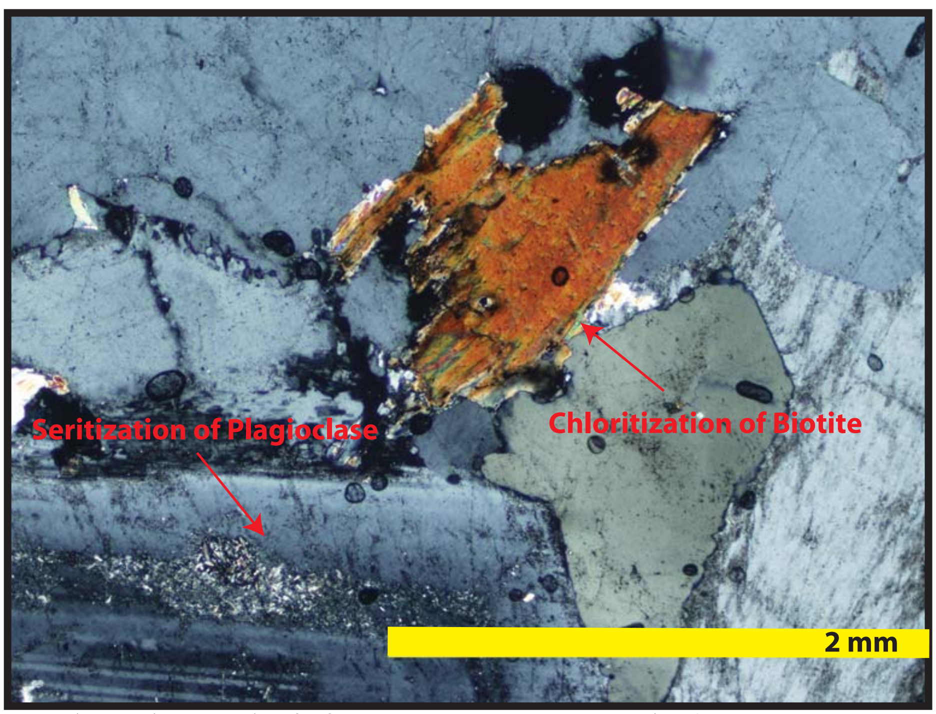

Figure 13: Photomicrograph of of Peggy's Cove Monzogranite (SCH-8, East Dover Rd.) showing alteration textures (seritization and chloritization) common in SMB granites. Cross polarized light.

Sandy Lake Monzogranite

Deep Cove

A thin section was made of a handsample (SCH-9), that was thought to contain garnet. The Sandy Lake Biotite Monzogranite is medium to coarse-grained and has the same modal percentages and textures as the Peggy's Cove Monzogranite. While garnet was not present in thin section, an epoxy mount prepared from the same hand sample contains anhedral garnets in a biotite clot that are texturally and compositionally similar to the garnet-rich biotite clots from the Peggy's Cove Monzogranite.

Contact Granodiorite

Handsamples were collected along a roadside outcrop of the biotite granodiorite unit mapped as the outermost unit of the Halifax Pluton (SCH-3, SCH-4, SCH-5). Thin sections show that the unit is medium- coarse grained. The biotite granodiorite consists of ~20% biotite with equal amounts of plagioclase, orthoclase, and quartz. Many of the feldspars have been partially or entirely altered to sericite. Some biotite displays chloritization. There is a small amount of muscovite (~1-2%) in all three thin sections as well as trace amounts of zircon, monazite, and illmenite. There are trace amounts of ~1-2mm subhedral to anhedral garnets in close association with both biotite and muscovite in all samples (Fig. 14). A sample (SCH-3) collected from a garnet-rich layer at the contact between the granodiorite and the Halifax formation country rock, contains the most garnet (Fig. 14).

BOOT LAKE PLUTON

Boot Lake Granodiorite

Three thin sections were prepared from handsamples collected from the Boot Lake granodiorite (SCH-12,SCH-17, SCH-18). They are medium to fine grained and contain equal amounts of quartz, orthoclase, and plagioclase with ~ 15-25% biotite. Chloritization of biotite and seritization of the plagioclase are common. Small amounts (~1%) of muscovite and illmenite are present in all samples. Garnet was not observed in one of the samples (SCH-12). The section is relatively fine grained and equigranular with a few larger feldspar and quartz crystals. SCH-17 contains an enclave of finer grained material with small subhedral garnets. SCH-18 contains subhedral to anhedral garnets that are larger (~ 2-3mm) than the surrounding groundmass (Fig 15).

SCRAG LAKE PLUTON

Scrag Lake Biotite Granodiorite

One thin section was prepared from a granodiorite handsample collected from the Scrag Lake Pluton (SCH-11). The thin section has ~20% biotite and equal amounts of plagioclase, orthoclase, and quartz and displays the same alteration textures as the granites of the Halifax Pluton (sertizied feldspars and chloritized biotites). The sample is medium grained but contains a fine-grained slightly more mafic and equigranular enclave. While small amounts of illmenite and muscovite (~1% each) were observed, no garnets were found.

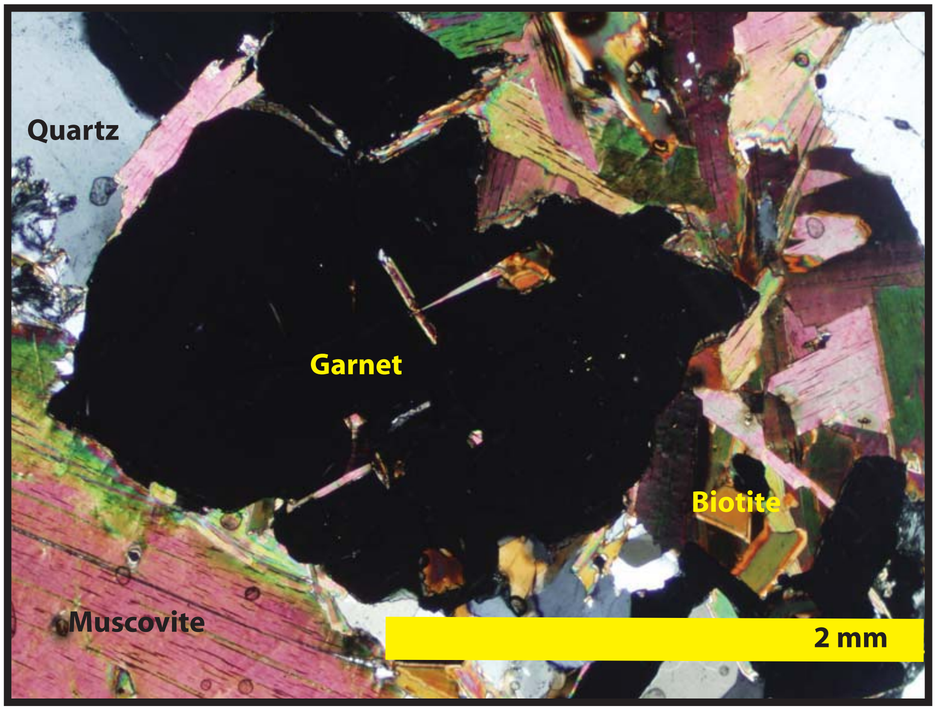

Figure 14: Photomicrograph of subhedral garnet surrounded by muscovite, biotite, and quartz. From garnet-rich layer in biotite granodiorite from the margin of the Halifax Pluton (SCH-3). Cross polarized light.

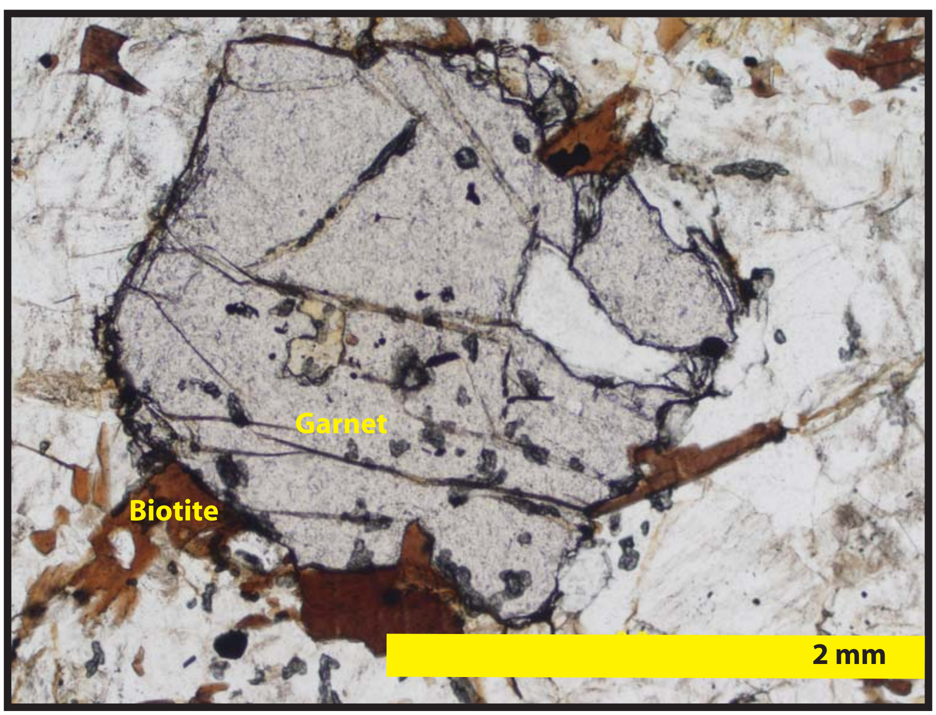

Figure 15: Photomicrograph of a fractured subhedral garnet in a fine grained biotite granodiorite collected in the highly contaminated Boot Lake Pluton (SCH-18). Plane light.

MEGUMA GROUP COUNTRY ROCKS

Goldenville Formation

A handsample collected from a roadside outcrop of the Goldenville Formation in the Halifax metro area was made into a thin section (SCH-1). The sample is a weakly metamorphosed greywacke. SCH-1 consists of quartz grains surrounded by a very- fine groundmass of miccaceous meta-sediments. Garnet was not observed in the Goldenville Formation: neither in the field nor in thin section.

Halifax Formation

A handsample was collected from the Halifax Formation at a roadside outcrop in the Halifax-metro area (SCH-2). Identifying minerals and modal percentages was difficult, given the very fine to fine grained texture of the rock. The unit is a meta-greywacke with quartz, plagioclase, orthoclase, biotite and muscovite with trace amounts of illmenite. No garnet was observed in the sample. Another handsample of the Halifax Formation collected from Upper Blanchford Rd (SCH-10) contains cordierite, pyrite, graphite and andalusite, some of which has been replaced by sillimanite (Fig 16).

A hornfels-facies garnet pelite was also collected near a Meguma Group-SMB contact on the margin of the Boot Lake pluton (SMB-15). Large euhedral (cm-scale) garnets are found in the sample and have thin biotite and muscovite coronas (Fig 17). There are quartz and illmenite inclusions in the garnet crystals. Some of the garnets have fine fractures that are filled with biotite and muscovite. A garnet from this sample was selected for the experimental portion of the study.

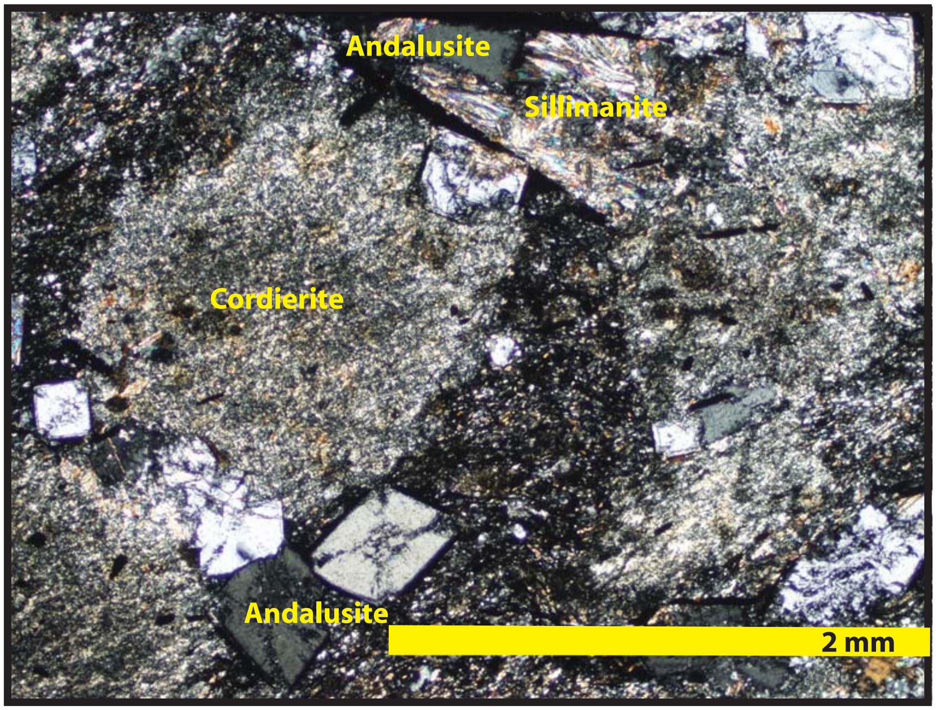

Figure 16: Photomicrograph of Halifax formation meta-greywacke (SCH-10). Cross polarized light. An andalusite crystal (top right) has been replaced by sillimanite.

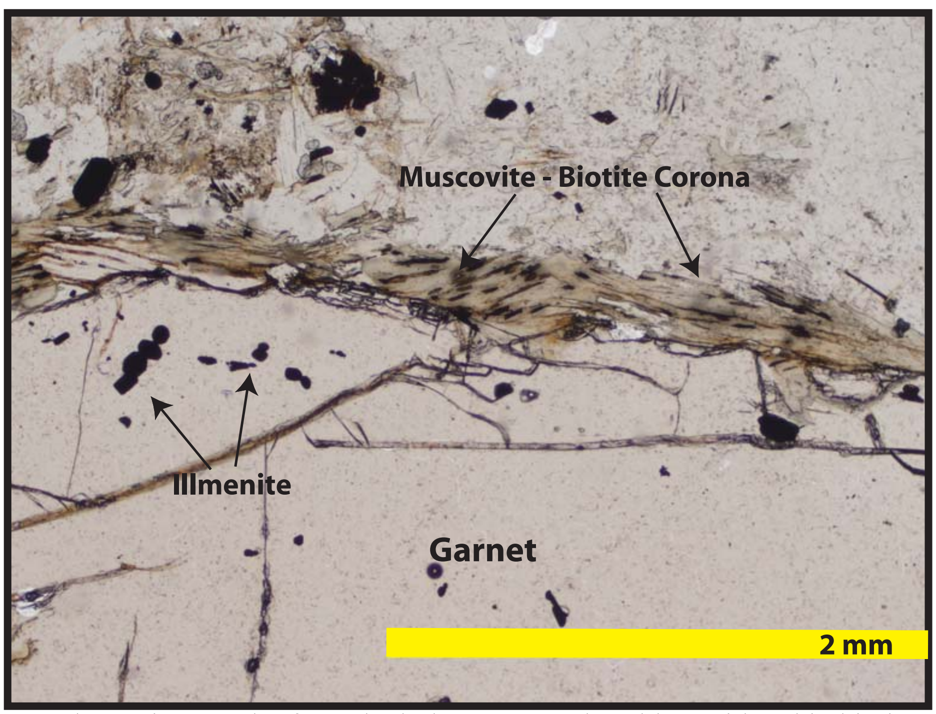

Figure 17: Photomicrograph of a euhedral garnet porphyroblast with a thin biotite and muscovite corona texture, fractures, and illmenite inclusions from sample SCH-18, Halifax Formation. Plane light.

CHAPTER 5: GARNET CHEMISTRY

METHODS

Garnets from twelve epoxy mounts and two thin sections were analyzed by scanning-electron microscopy with energy dispersive x-ray spectrometry (SEM/EDS). The SEM was used to observe the textures of the garnets in the epoxy mounts and to identify inclusions and the surrounding grains. Compositional profiles, maps, and quantitative analyses of garnet cores and rims were used to determine the zonation of cations within individual garnet crystals. (SEM analyses of SMB garnets can be found in Appendix A.)

RESULTS

Backscattered electron images show small anhedral (≤ 2mm) garnets closely related to biotite in all samples. Illmenite, quartz, and biotite are common inclusions in the garnets (Figure 18, A). SEM/EDS analyses show that SMB garnets are almandine-rich, with spesssartine enriched rims. This is consistent for the Halifax and Boot Lake Plutons (Figure 19). Garnet cores consistently have higher concentrations of Fe and Mg than garnet rims. Profiles across garnets show that the rims of the garnets are ~.2mm in width (Figure 20). Compositional maps of garnets show that the manganese rims follow the anhedral form of the garnets (Figure 18B).

Garnets from metamorphic environments with spessartine-rich cores and almandine rims are considered normally zoned (Deer et al., 1982). These garnets are thought to have formed during prograde metamorphism, whereby spessartine-rich garnet will form first because it is stable at lower temperatures. Garnets of the South Mountain

Batholith are reversely zoned; thus, their zonation must result from mechanisms different from those resulting typical of prograde metamorphism.

The Mn rims around the garnets are evidence of a chemical interaction between xenocrystic garnets and a granite melt. The Mn may have diffused into the xenocrystic garnet from the peraluminous granite melt, as the garnet equilibrated with the magma. Another possibility is that the source of the Mn was not the granite melt, but the garnet itself; the Mn may have preferentially stayed behind and diffused into the remaining garnet as the crystal partially melted. A third hypothesis is that the garnets are Avalonian metamorphic garnets with Mn rims produced during the partial melting that produced the SMB.

A.

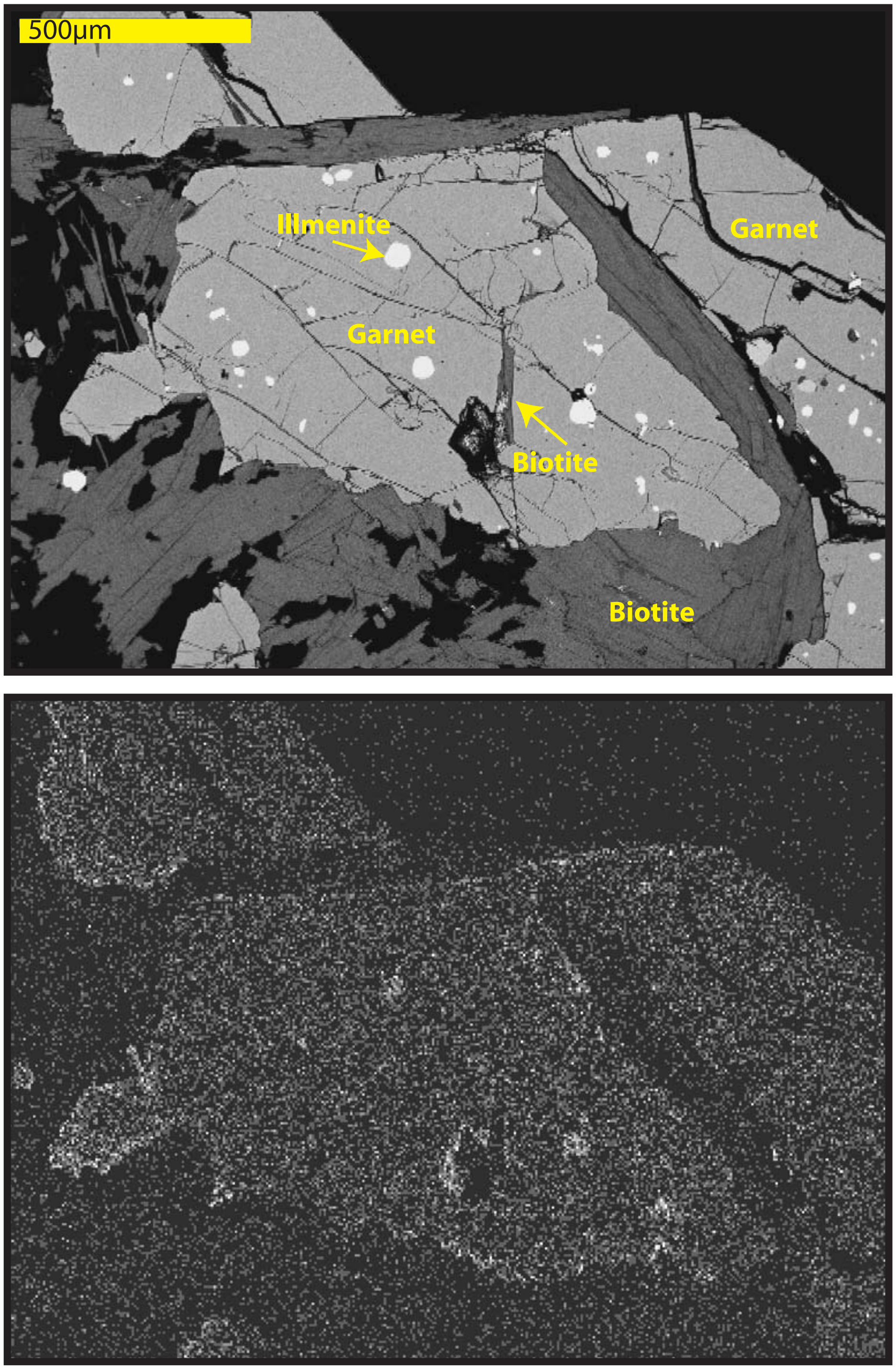

B.

Figure18: (A) Backscattered electron image of garnet in a biotite clot (SCH-26) from the Peggy's Cove Monzogranite collected at Cranberry Head.The garnet at the center of the image is anhedral, fractured and contains illmenite and biotite inclusions. (B.) Compositional map of Manganese in the same garnet sown in A. The Mn rim follows the anhedral form of the crystal.

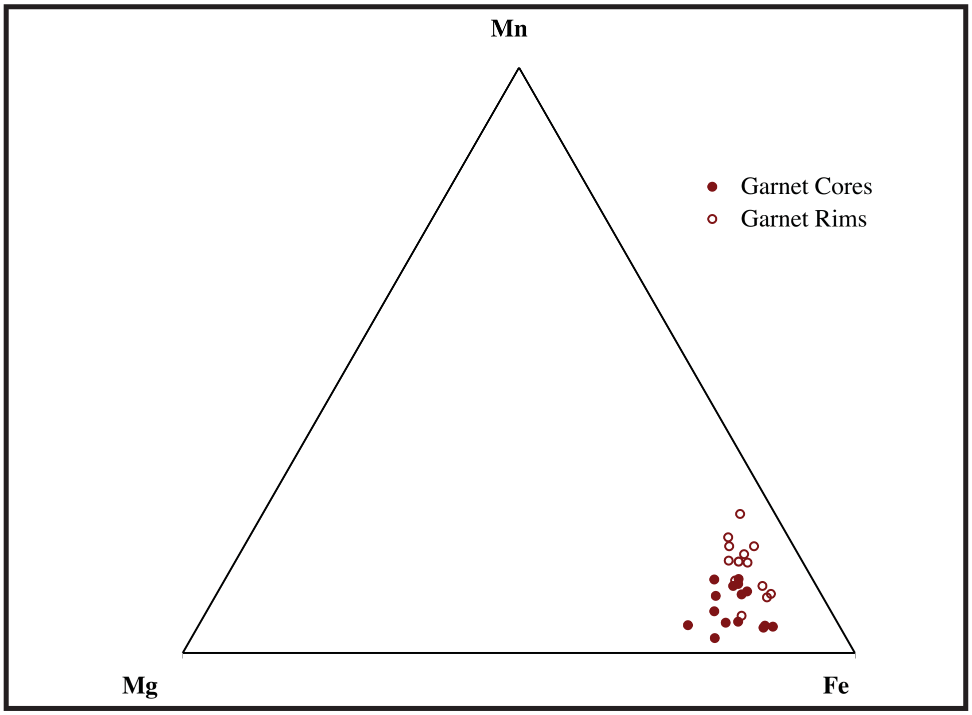

Figure 19: Ternary diagram showing average core and rim compositions for SMB garnets (in mole units). All garnets are almandine rich with spessartine enriched rims.

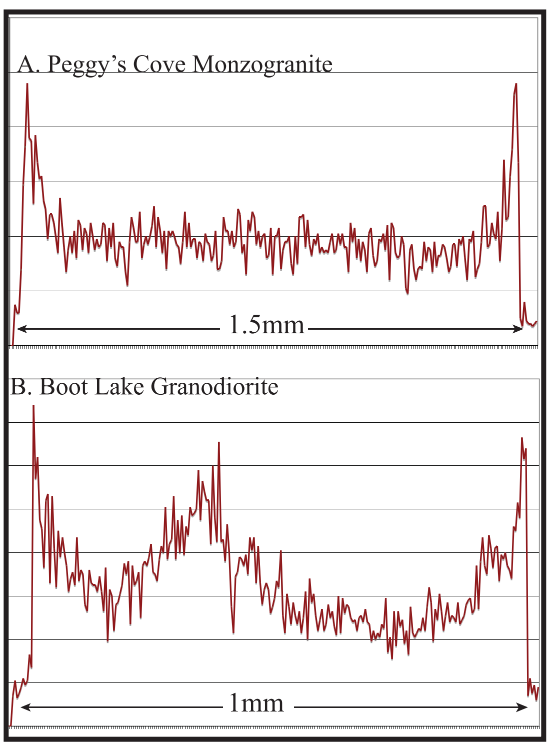

Figure 20: Mn profiles across garnet from Peggy's Cove Monzogranite (A) and Boot Lake Granodiorite (B). The peak in the middle of B corresponds to an illmenite inclusion.

CHAPTER 6: EXPERIMENTS

RATIONALE

Experiments were conducted to determine the reactivity of Meguma garnets in the Peggy's Cove monzogranite. The goal of the experiments is to see if xenocrystic metamorphic garnets are likely to experience resetting of major and minor cations by diffusional re-equilibrium as they sit in a peraluminous granite magma at a high temperature. The experiments are an analog to see if Meguma garnet xenocrysts dissolve, grow, or exchange with a peraluminous magma.

PROCEDURE

Glasses were prepared from a sample of Peggy's Cove Monzogranite collected at Cranberry Head by Kendra Murray (SMB12). The granite was first crushed by Kendra Murray with a jaw cruncher and possible metal chips from the crusher were removed with a magnet. The crushed sample was then ground with a tungsten carbide mortar and pestle to a fine powder and heated to 1300 °C at 10 kb in graphite and quenched after two hours to form glass (Fig. 21). A garnet crystal from a Meguma Group garnet pelite in the Boot Lake area (SMB-15) was cut and polished. Slices of this garnet were surrounded by a powder of the Peggy's Cove Monzogranite glass and sealed in a gold tube with two different concentrations of water (5% and 10% by mass), to make up for the dehydration that took place when the glass was made (Fig 22).

Figure 21: Photo of glass sample inside a graphite crucible, prepared from a sample of Peggy's Cove Monzogranite collected at Cranberry Head

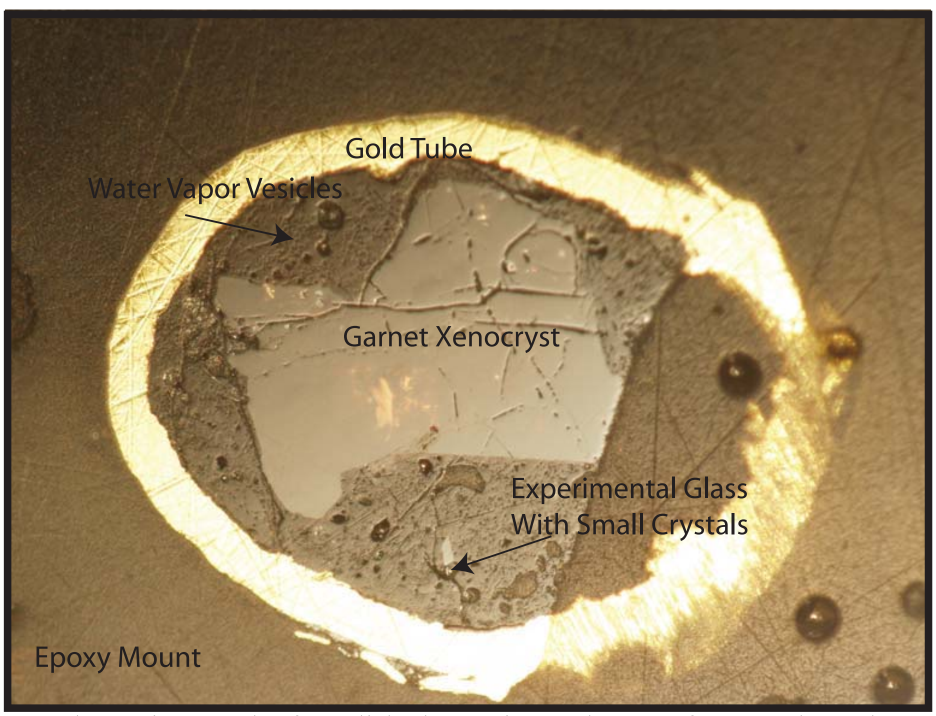

Figure 22: Photomicrograph of a polished experimental garnet from run heated to 700 °C. Diameter of the gold tube is ~2mm.

All the experiments were conducted with a piston-cylinder apparatus in the Experimental Petrology Lab at Smith College. Two small (~2mm in diameter) holes were drilled in a graphite rod to make a crucible for the gold tubes. The graphite crucible was covered with a <1 mm graphite lid and placed inside a fired pyrophyllite cup with lid, inside a graphite furnace with MgO spacers above and below the crucible (Morse, 2004). The furnace was surrounded by a pyrex tube, halite sleeve, and a layer of lead foil before it was placed inside the cylinder. Thermocouple wires were fed through a base plug inside a pyrophyllite sleeve and rested on top of the fired pyrophyllite cap. The samples were then pressurized hydraulically and heated to experimental temperatures.

Successful runs were conducted at 5 kb and two temperatures (800 °C and 700 °C). The first experiment was run at 800 °C for two days. The second experiment was run at 700 °C for three and a half days. Experimental results were analyzed on the SEM to test the hypothesis that Mn is either diffusing into the garnet as it reacts with the granite or it is concentrating in the rim of the garnet as it partially melts in the granite. (SEM analyses of experiments can be found in Appendix B.)

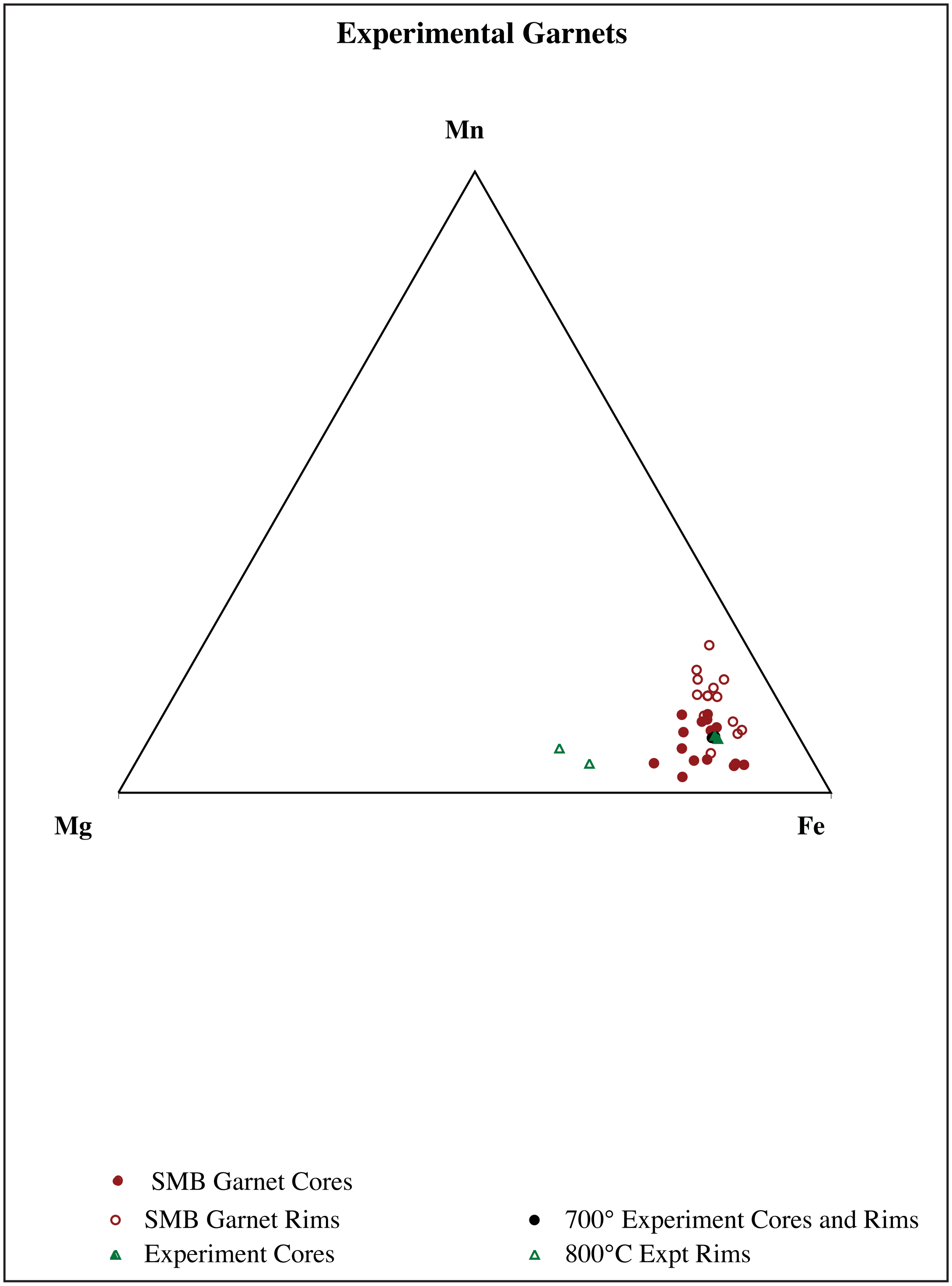

Figure 23: Ternary plot of experiment garnets from the two runs with SMB garnets. The run at 800°C produced Mg-enriched overgrowths, garnet rim compositions equal garnet core compositions at 700°C. (Compositions plotted in mole units)

RESULTS

The Mn-enriched rims observed in the SMB garnets were not reproduced by the first experiment at 800 °C (Fig. 23). New Mg-rich garnet overgrowths were observed in both samples (Fig. 24). Facets were observed in garnet overgrowths on the Boot Lake garnets (Fig. 24). Small crystals formed in the melt, which was again quenched to form glass (Figure 25). Chemical analyses show that most of these small crystals are orthopyroxene and biotite with some illmenite. The biotite and orthopyroxene commonly group together in an H pattern (Figure 25). Holes in the surrounding glass are evidence of an H_2O-rich liquid phase and represent a vapor phase formed from water that was added to the system in excess of the quantity that could dissolve in the melt. The experimental results at 800 °C may be different from SMB garnets because they were heated to a higher temperature (to enhance reaction kinetics) than what may be expected for SMB granites, thus a run was conducted at 700 °C.

The second run (at 700 °C) showed the garnet xenocryst dissolving in the peraluminous melt. The texture of a polished face of the garnet xenocryst was rough and disaggregated (Fig. 26). A large hole had formed in the garnet and was filled with small biotite crystals (Fig. 27). Biotite, quartz, plagioclase and illmenite are the phases present in the glass around the garnet xenocryst (Fig. 28). Holes in the glass again showed an H_2O-rich liquid phase was present (Fig. 28). The garnet did not have spessartine enriched rims; no strong zonations were observed in the garnet xenocryst (Fig. 23).

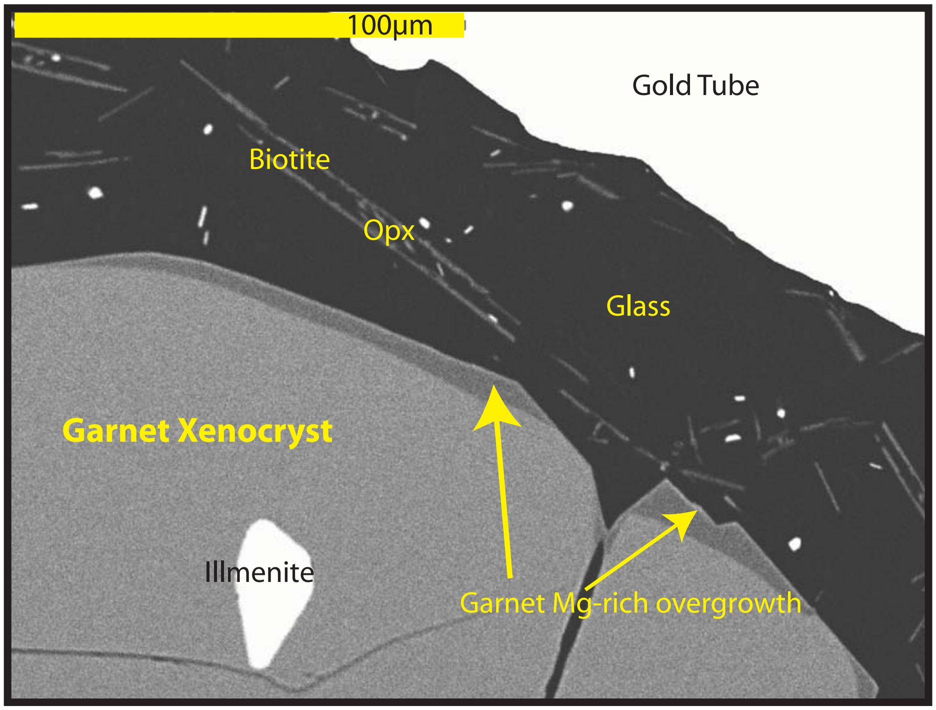

Figure 24: Backscattered electron image of an experimental garnet with a Mg-rich overgrowth and new crystal facets.

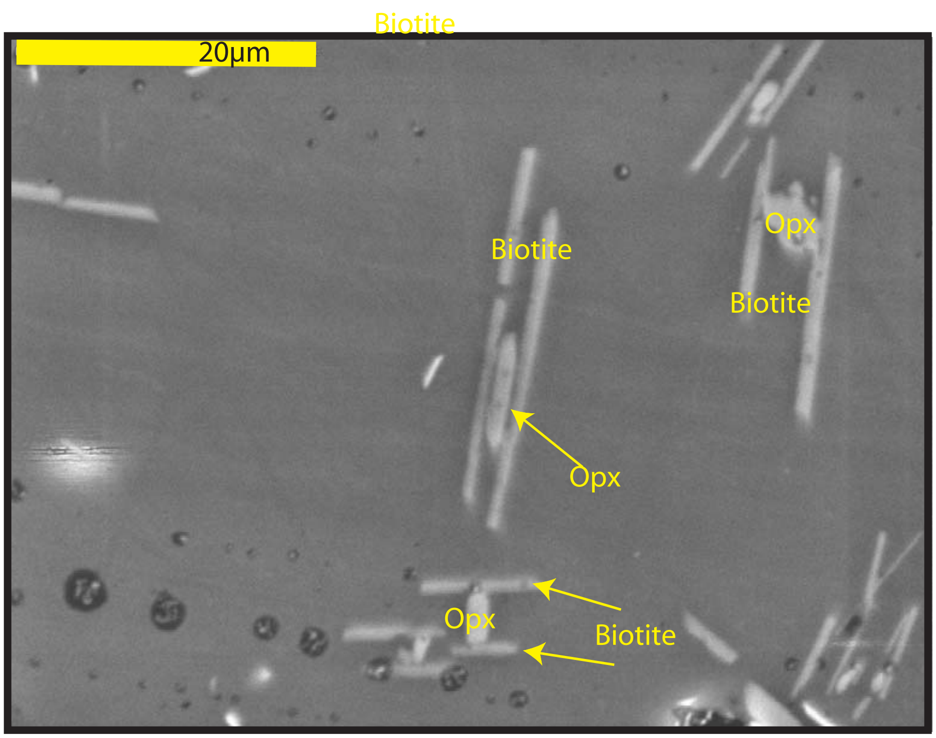

Figure 25: Backscattered electron image of biotite-orthopyroxene crystals. Orthopyroxene crystals occur between two parallel biotite crystals.

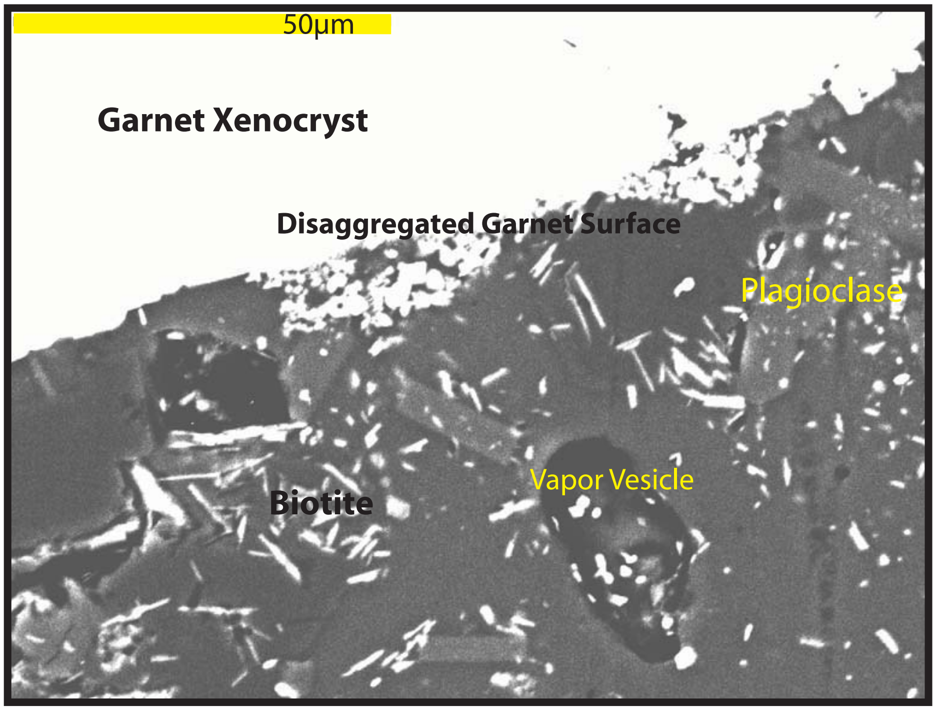

Figure 26: Backscattered electron image of garnet dissolving in the Peggy's Cove Monzogranite.

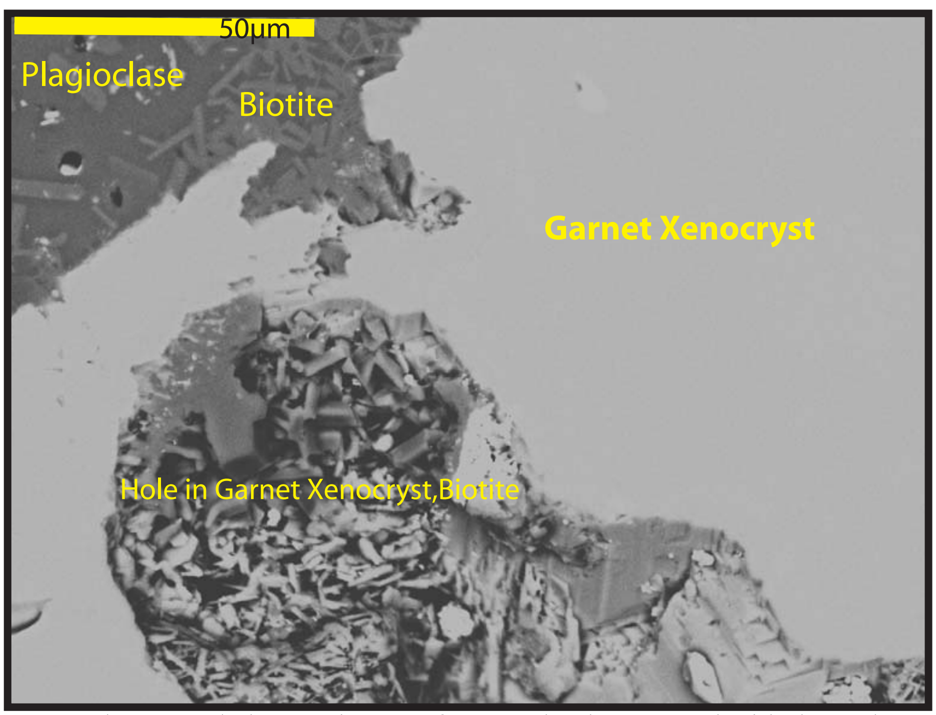

Figure 27: Backscattered electron image of garnet that has reacted with the melt to produce biotite. The hole in the center of the image shows where biotite has replaced the garnet.

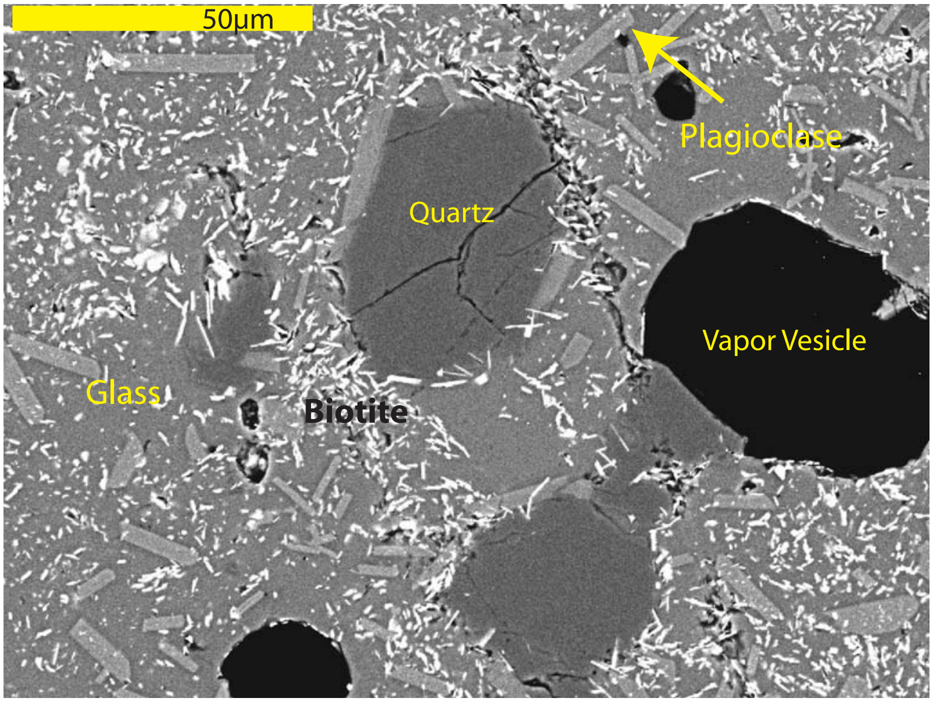

Figure 28: Backscattered electron image of quartz, plagioclase, and biotite in the experimental glass. Holes are evidence of a vapor phase.

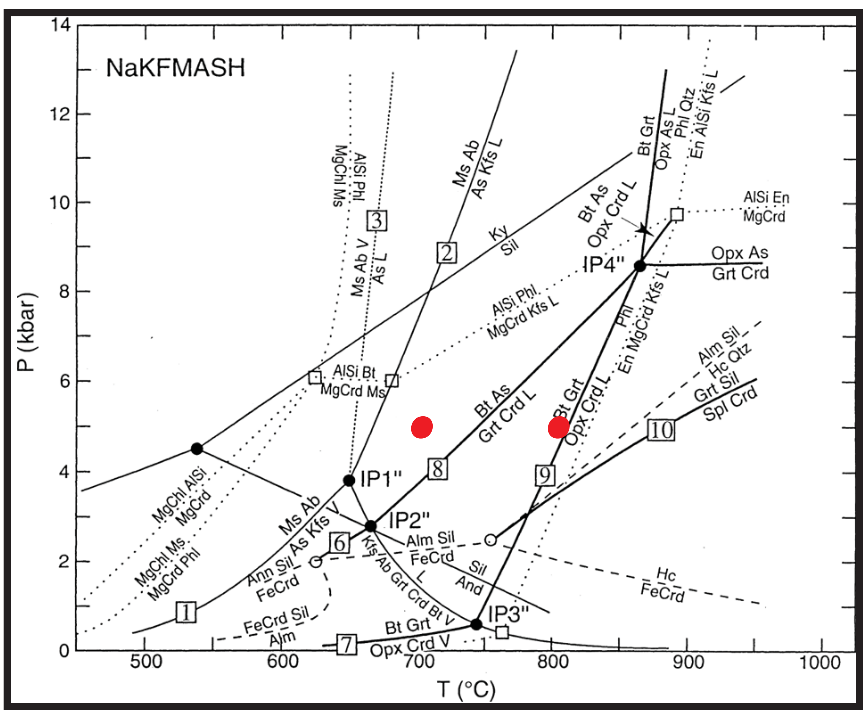

Figure 29: Possible melting reactions for experiment systems (modified from Spear et al., 1999). At 800 °C, garnet precipitated from the melt. At 700°C , the garnet dissolved. These results are consistent with model reactions 8 and 9.

Experimental results are consistent with model pelite melting reactions from a similar NaKFMASH system (Spear et al., 1999) (Fig. 29). At 800 °C, garnet precipitated from the melt forming Magnesium rich overgrowths on the xenocryst. At 700 °C the garnet dissolved and reacted with the melt to produce biotite. The results from 700 °C support our hypothesis that a garnet xenocryst could be resorbed in a peraluminous granite melt. It is likely that spessartine rich rims didn't develop during resorption in the experiment because it wasn't run long enough; there was not enough time for a measurable amount of Mn to diffuse back into the crystal. It is possible that the garnet xenocrysts were picked up by the melt when its temperature was below 800 °C, because the 700 °C results show that garnet didn't grow. It is possible that garnets xenocrysts may have grown during the intrusion of the SMB and that any growth present was lost during cooling and dissolution.

CHAPTER 7: DISCUSSION AND CONCLUSION

DISCUSSION

Garnets in the granitoids of the South Mountain Batholith in the Halifax and Boot Lake Plutons are most likely xenocrysts from the metamorphic rocks that host the granites. This is based on the close field relationships of garnet with xenoliths, garnet chemistry (reverse zoning), the results of the experiments, and a consistent lack of textural and chemical equilibrium between garnet crystals and their host rocks. Xenocrysts derived from partially assimilated metamorphic rocks have been previously been suggested as an origin for garnets in granitic rocks (Warren, 1970).

Possible modes of origin of garnet xenocrysts in a peraluminous melt are shown in Figure 30. Our results show that garnet came into contact with the melt as country rocks were being digested by the intruding SMB. Psammite and pelite country rocks partially melted in the magma. Garnet crystals took on an anhedral form as they were resorbed by reaction with the granite liquid. The biotite clusters in which most of the garnet occurs are textural evidence for disequilibrium of garnet with SMB granites. Experiments show that these clots can be produced as the Meguma Group metamorphic garnet reacts with peraluminous melt to produce biotite. The production of a biotite halo may have protected the garnet from completely dissolving in the granite. During resorption, Mn diffused into the garnet creating spessartine-enriched rims. A diffusion calculation ($x = \mathrm{Sqrt}[Dt]$) using the Mn diffusivity for almandine of Chakrabotry and Ganguly (1992) shows that the size of the observed Mn rims (~.2 mm) could have been produced by diffusion in a reasonable amount of time , ~1 millon years at 700°C, and 100,000 years at 800°C.

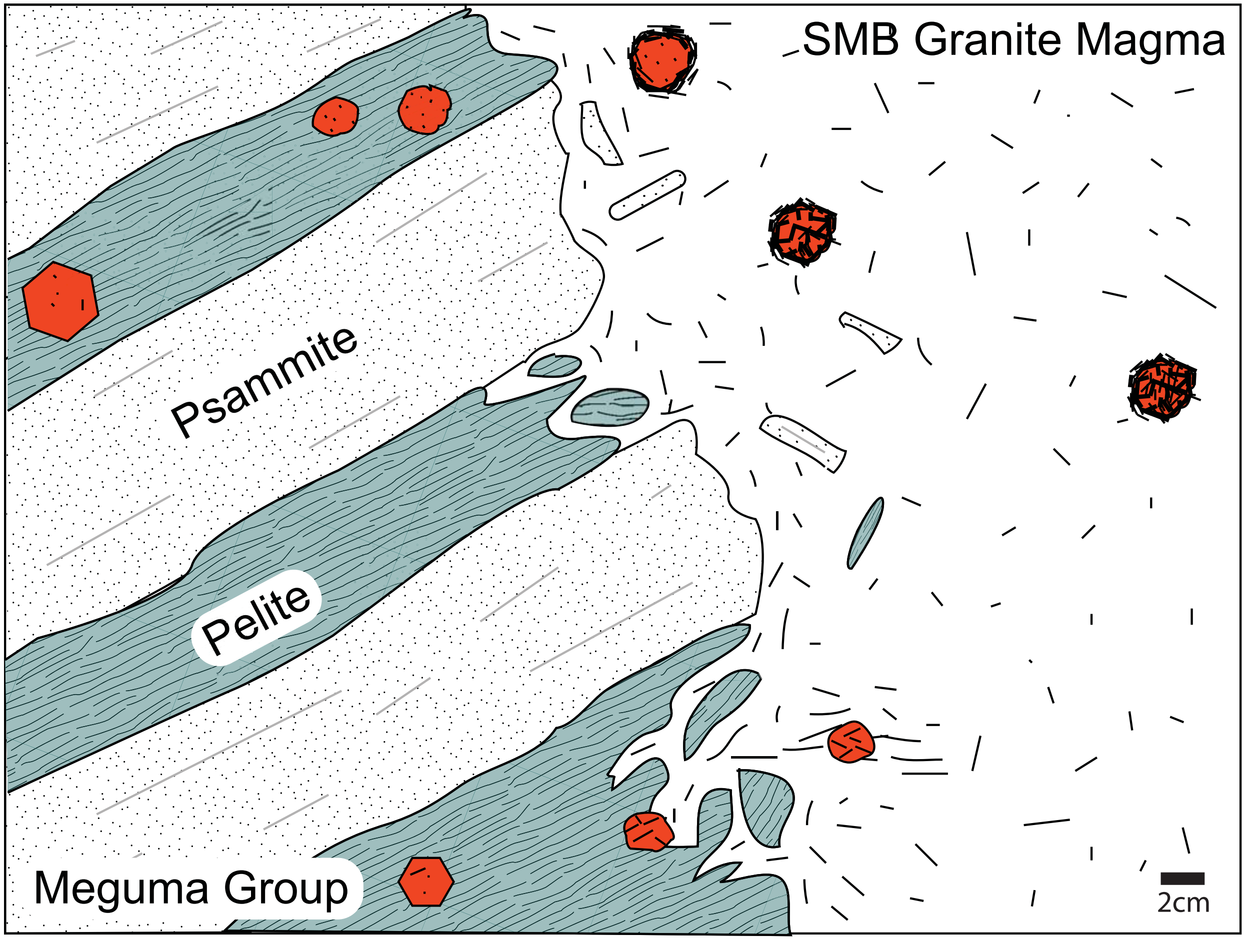

Figure 30: Modes of origin of a garnet xenocryst in a peraluminous granite melt showing garnets from Meguma Group country rocks coming into contact with the SMB melt, partially melting, and reacting to form an Mn rim and a biotite halo (Modified from Lackey, 2007).

There are two possible sources for xenocrystic garnets in SMB granites: Meguma Group country rocks or the rocks of the Avolonian Basement, which is thought to be the rock that partially melted to form the SMB (MacDonald, 2001). The Meguma Group seems to be the most likely source for garnet. At Boot Lake, garnet was found in close association with clusters of biotite and garnet. Some garnet biotite clots appear to be trailing out of partially melted Meguma xenoliths and becoming entrained in the granite (Fig. 10). Garnet was also found in abundance at the contact between the granodiorite of the Halifax Pluton and the Meguma Group at a roadside outcrop in the Halifax Metro area (Fig. 8). Avalonian basement rocks may be another possible source for garnets. While there is no field evidence to suggest this, Hark (2007) notes that there is isotopic evidence for Avolonian Garnets in the SMB and proposes that high $\delta^{18}O$ in garnets may correspond to a lithology of a higher $\delta^{18}O$ than measured for the Meguma Group (perhaps the Avalonian Basement).

Garnet occurrences in the SMB and other peraluminous granite bodies have previously been explained by processes that are inconsistent with the findings of this study. Kontak (1998) reports garnets of a metsomatic origin in the Big Indian Polyphase Intrusive body of the SMB. Big Indian Polyphase Intrusive garnets occur as euhedral to subhedral single grains, in quartz clots, and have an antipathetic relationship to biotite (Kontak, 1998). Garnets from the Boot Lake and Halifax Plutons bear no textural resemblance to the BIPI garnets and clearly are not the result of a post-magmatic interaction between hydrothermal fluids with host granitoids. Subsolidus garnets that have been observed in SMB aplites may have formed by processes similar to those reported by Kontak (1998) (Jade Star Lackey, personal communication). No such garnets were observed or collected in this study.

While the possibility of magmatic garnets in the SMB has been suggested, and a single euhedral garnet was observed at East Dover Road, there is little textural evidence for the garnets considered in this study to have nucleated and grown in the granite melts of the Batholith.

The role of Mn in the stabilization of garnets in granite has been emphasized in several studies (Green, 1976; Miller and Stoddard, 1981; duBray 1988); therefore, it was important to consider the Mn content of SMB garnets and their host rocks before ruling out the possibility of magmatic garnets. Miller and Stoddard (1981) attribute the presence of magmatic garnet in the peraluminous rocks of the Old Woman-Piute Range to late stage Mn-enrichment that took place as the granite bodies became more differentiated. The garnets considered in their study were poorly zoned and had a much higher spessartine component than the garnets collected in the Boot Lake and Halifax Plutons. Their garnets are euhedral, inclusion poor or free, up to 5mm across and appeared to be in textural equilibrium with the granite. Miller and Stoddard conclude that the garnets precipitated in response to an increased ratio of Mn/Fe+Mg with differentiation.

duBray describes garnets from the peraluminous granites of the southeastern Arabian Shield (1988). They contain more spessartine and less pyrope then SMB garnets, but they are reversely zoned with spessartine enriched rims and more almandine-pyrope rich cores. These garnets were small (~1mm in diameter), subhedral, and inclusion free. While most were in textural equilibrium with the other minerals of the granites, samples from the Madha pluton were reported to be, "adjacent to biotite and appear to have been growing at the expense of biotite and an inverse –abundance relation exists between garnet and biotite." They suggest that, "the small size and relatively poor (subhedral) form of the garnet crystals imply crystallization relatively late in the solidification process." duBray attributes the reverse zoning (spessartine rims and almandine cores) to normal magmatic processes whereby melt-phase manganese enrichment develops during differentiation.

SMB garnets and granites are relatively Mn-poor compared to those reported by du Bray (1998) and Miller and Stoddard (1981). The amount of spessartine in SMB garnets is much lower than garnets thought to be of a magmatic origin. SMB garnets have cores that range from 3-11% spessartine and rims that are 7- 23% spessartine. Miller and Stoddard report garnets with cores that are 42% spessartine and rims that are 35%. duBray reports garnets that contain as much as 66% spessartine (Fig. 31). The granites of the Halifax and Boot Lake Plutons are not highly differentiated or enriched in Mn. The molar ratio of Mn/Fe+Mg in SMB granites is consistently 0.02. (Mumaw and Murray, 2007 – full XRF analyses for Boot Lake granodiorite and Peggy's Cove Biotite Monzogranite can be found in Appendix C.) Miller and Stoddard suggest that the formation of magmatic garnets is likely in granites with ≥0.04 molar Mn/Fe+Mg. There is no textural or chemical evidence to suggest that the Mn-enrichment by magmatic differentiation led to the nucleation of the garnets in the Halifax and Boot Lake Plutons; this further supports our hypothesis that the garnets of the SMB are xenocrysts.

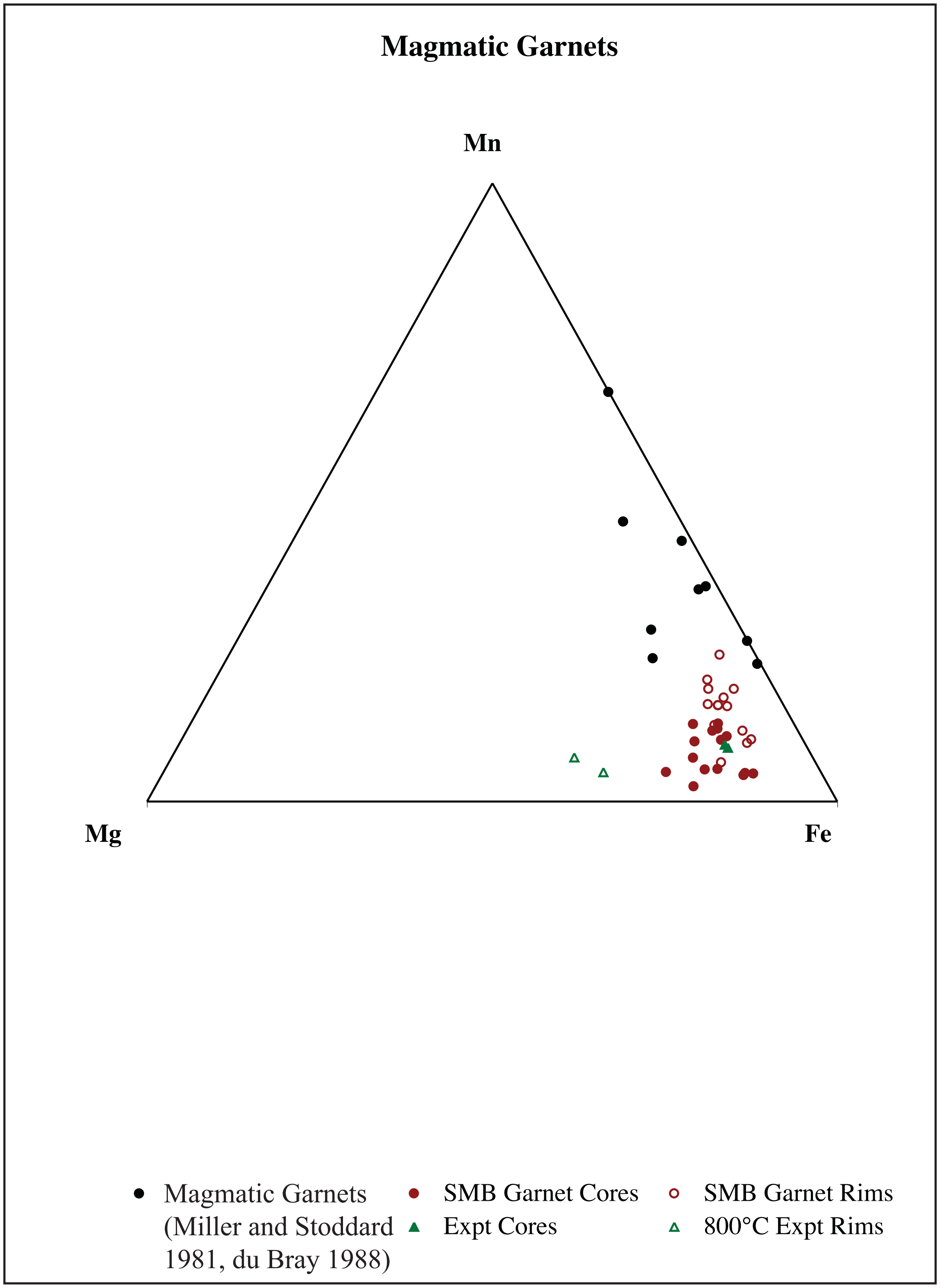

Figure 30. Ternary diagram showing a higher spessartine content in magmatic garnet then in SMB and experimental xenocrystic garnets. Magmatic garnets reported by Miller and Stoddard (1981) and du Bray (1998). (Composition reported in mole units)

A study of metapsammitic and metapelitic contaminants from the Meguma Group country rocks in the SMB was conducted by Erdmann and Clarke (2007). They suggest that metapelitic rocks of the Meguma Group in the SMB partially melted to a high degree, releasing peritectic garnets into the partial melts of the SMB. Erdmann and Clarke interpret the garnet-rich layers found at SMB and Meguma contact zones, such as the granodiorite-Meguma contact on the margin of the Halifax Pluton, to be the result of extensive assimilation of metapelitic country rocks (Erdman and Clarke, 2007). This is further evidence to support a xenocrystic origin for garnet and also confirms that a source for garnet xenocrysts is the Meguma Group country rocks.

CONCLUSIONS

Garnet in the marginal units of the Halifax and Boot Lake Plutons in the South Mountain Batholith, Nova Scotia are xenocrystic in origin. Their reverse Mn zonation and relationship with biotite suggests a partial assimilation of country rocks with the intruding SMB magma. The character of the SMB garnets considered in this study shows that the SMB magma reacted with pockets of country rock but didn’t equilibrate entirely. While garnet was not entirely consumed by reaction with the SMB magma, the xenoliths that once hosted the crystals may have preferentially been digested in the SMB. The results of this study imply limited magma mixing between the SMB magmas and partially melted Meguma Group country rocks

References:

Allan, B.D. and Clarke, D.B., 1981, Occurrence and origin of garnets in the South Mountain Batholith, Nova Scotia: The Canadian Mineralogist, v.19, pp. 19-24.

Benn, K., Roest, W. R., Rochette, P., Evans, N. G., and Pignotta, G. S., 1999, Geophysical and structural signatures of syntectonic batholith construction; the South Mountain Batholith, Meguma Terrane, Nova Scotia: Geophysical Journal International, v. 136, no. 1, pp. 144-158.

Chakraborty, S. and Ganguly, J., 1992, Cation diffusion in aluminosilicate garnets: experimental determination in spessartine-almandine diffusion couples, evaluation of effective binary diffusion coefficients, and applications: Contributions to Mineralogy and Petrology, v. 111, pp 74-86.

Clarke, D. Barrie, MacDonald, Michael A., and Erdmann, Saskia, 2004, Chemical variation in Al2O3-CaO-Na2O-K2O space: controls on the peraluminosity of the South Mountain Batholith: Canadian Journal of Earth Science., v. 41, pp.785-798.

Deer WA, Howie RA, Zussman J (1982) Rock-Forming Minerals, Volume 1A-Orthosilicates. Longman, New York, p 919

du Bray, Edward A., 1988, Garnet compostions and their use as indicators of peraluminous granitoid petrogenesis- southeastern Arabian Shield: Contributions to Mineralogy and Petrology, v.100, pp. 205-212.

Erdmann, Saskia, London, David, Morgan VI, George B., and Clarke, D. Barrie, 2007, The Contamination of Granitic Magma by Metasedimentary Country-Rock Material: An Experimental Study: The Canadian Mineralogist, v. 45, pp. 43-61.

Erdmann, S., and Clarke, D.B., 2006, Nature and significance of metapsammitic and metapelitic contaminants in the peraluminous South Mountain Batholith: Lithos (in press)

Green, T.H., 1976, Experimental generation of cordierite-or garnet-bearing granitic liquids from a pelitic composition: Geology, pp. 85-88.

Green, T.H., 1977, Garnet in Silicic Liquids and Its Possible Use as a P-T Indicator: Contributions to Mineralogy and Petrology, v.65, pp.59-67.

Hark, Jessica, 2007, An Oxygen Isotope Study of the Garnet in the Peraluminous South Mountain Batholith Nova Scotia: Proceedings of the 20th Annual Keck Symposium, pp. 249-254.

Keppie, J. D., 1993, Synthesis of Palaeozoic deformational events and terrane accretion in the Canadian Appalachians: Geologische Rundschau, v. 82, no. 3, p. 381-431.

Kontak, Daniel J., and Corey, Michael, 1988, Metasomatic Origin of Spessartine-Rich Garnet in the South Mountain Batholith, Nova Scotia: Canadian Mineralogist, v. 26, pp. 315-334.

Kontak, Daniel J., Dostal, Jaroslav, Kyser, T. Kurt, and Archibald, Douglas A., 2002, A Petrological, Geochemical, Isotopic and Fluid-Inclusion Study of 370 Ma Pegmatite-Aplite Sheets, Peggys Cove, Nova Scotia, Canada: The Canadian Mineralogist, v.40, pp. 1249-1286.

Lackey, J.S., Erdmann, S., Clarke, D.B., Fellah, K.L., Nowak, R.M., Spicuzza, M., and Valley, J.W., 2006b, Oxygen isotope evidence for the origins of garnet in the peraluminous South Mountain Batholith, Nova Scotia: Geological Society of America, Annual Meeting, Philadelphia, Pennsylvania, Abstracts, paper 41-11.

Leake, BE (1967) Zoned garnets from the Galway granite and its aplites. Earth Planet Science Letters 3:311-316

MacDonald, M. A., 2001, Geology of the South Mountain Batholith, southwestern Nova Scotia, Department of Natural Resources - Mineral Resources Branch, Open File Report ME 2001-002.

Miller, Calvin F., and Stoddard, Edward F., 1981, The Role of Manganese in the Paragenesis of Magmatic Garnet: An Example from the Old Woman-Piute Range, California: Journal of Geology, v. 89, pp. 233-246.

Morse, S.A., Brady, J.B., and Sporleder, B.A., Experimental Petrology of the Kiglapait Intrusion: Cotectic Trace for the Lower Zone at 5 kbar in Graphite: Journal of Petrology, v. 45, pp2225-2259

Mumaw, Brian., 2007, The Contamination History of the Boot Lake Granodiorite, Nova Scotia: Proceedings of the 20th Annual Keck Symposium, pp. 262-268.

Murray, K.E., 2007, Using $\delta^{18}O$ of zircon and geochemistry to determine the magmatic evolution and degrees of contamination in the Peggy's Cove monzogranite, Halifax Pluton, Nova Scotia: Senior Integrative Exercise, Carleton College.

Murphy, J. Brendan, and Keppie, J. Duncan, 2005, The Acadian Orogeny in the Northern Appalachians: International Geology Review, v. 47, pp. 663-687.

Spear, Frank S., Kohn, Matthew J., and Cheney, John T., 1999, P-T paths from anatectic pelites: Contrib Mineral Petrol, v. 134, pp. 17-32.

Warren, R.C., 1970, Electron microprobe investigations of almandine garnets from a quartz diorite stick and adjacent metamorphic rocks, British Columbia: EOS, v.51, p.444.

Grt 1.1	core	SCH-15													
Elmt	Line	Spectrum	Apparent conc.	Stat. Sigma	k Ratio	k Ratio Sigma	Fit Index	Inten. Corrn.	Std. Corrn.	Element %	Sigma %	Atomic %		Compound %	Nos. of ions
Mg	K	ED	1.07	0.05	0.04	0.00	0.42	0.69	1.00	1.56	0.07	1.58	MgO	2.58	0.32
Al	K	ED	9.53	0.10	0.71	0.01	1.13	0.84	1.00	11.29	0.12	10.29	Al2O3	21.33	2.06
Si	K	ED	14.89	0.11	0.47	0.00	0.46	0.88	1.00	16.96	0.13	14.86	SiO2	36.29	2.97
Ca	K	ED	0.81	0.05	0.04	0.00	0.20	0.96	1.00	0.84	0.05	0.52	CaO	1.18	0.10
Mn	K	ED	4.00	0.13	0.12	0.00	0.40	0.99	1.00	4.04	0.13	1.81	MnO	5.22	0.36
Fe	K	ED	23.77	0.28	0.45	0.01	0.86	0.96	1.00	24.82	0.29	10.94	FeO	31.93	2.19
O	Ka	ED								39.01	0.25	60.00			12.00
			Cation sum 0.00												
* = <2 Sigma															
Grt 1.2	core	SCH-15													
Elmt	Line	Spectrum	Apparent conc.	Stat. Sigma	k Ratio	k Ratio Sigma	Fit Index	Inten. Corrn.	Std. Corrn.	Element %	Sigma %	Atomic %		Compound %	Nos. of ions
Mg	K	ED	1.85	0.08	0.14	0.01	0.86	0.86	1.00	2.16	0.10	2.15	MgO	3.59	0.43
Al	K	ED	8.79	0.09	0.46	0.00	1.48	0.78	1.00	11.27	0.11	10.08	Al2O3	21.29	2.02
Si	K	ED	16.01	0.12	0.57	0.00	0.56	0.93	1.00	17.20	0.13	14.78	SiO2	36.79	2.96
Ca	K	ED	0.96	0.06	0.07	0.00	0.13	1.04	1.00	0.92	0.05	0.56	CaO	1.29	0.11
Mn	K	ED	4.13	0.13	0.12	0.00	0.42	0.99	1.00	4.18	0.13	1.84	MnO	5.40	0.37
Fe	K	ED	23.63	0.27	0.45	0.01	0.43	0.96	1.00	24.69	0.29	10.67	FeO	31.76	2.14
O	Ka	ED								39.70	0.26	59.91			12.00
			Cation sum 0.00												
* = <2 Sigma															
Grt 1.3	rim	SCH-15													
Elmt	Line	Spectrum	Apparent conc.	Stat. Sigma	k Ratio	k Ratio Sigma	Fit Index	Inten. Corrn.	Std. Corrn.	Element %	Sigma %	Atomic %		Compound %	Nos. of ions
Mg	K	ED	1.16	0.08	0.09	0.01	0.30	0.85	1.00	1.36	0.09	1.39	MgO	2.26	0.28
Al	K	ED	8.67	0.09	0.45	0.00	0.28	0.78	1.00	11.08	0.11	10.19	Al2O3	20.94	2.04
Si	K	ED	15.59	0.12	0.56	0.00	0.49	0.93	1.00	16.70	0.13	14.75	SiO2	35.72	2.95
Ca	K	ED	0.98	0.06	0.07	0.00	0.29	1.04	1.00	0.94	0.05	0.58	CaO	1.31	0.12
Mn	K	ED	5.80	0.14	0.17	0.00	0.74	0.99	1.00	5.86	0.15	2.65	MnO	7.57	0.53
Fe	K	ED	22.70	0.27	0.43	0.01	0.99	0.96	1.00	23.66	0.28	10.51	FeO	30.43	2.10
O	Ka	ED								38.64	0.26	59.92			12.00
			Cation sum 0.00												
* = <2 Sigma															
Grt 2.1	rim	SCH-15													
Elmt	Line	Spectrum	Apparent conc.	Stat. Sigma	k Ratio	k Ratio Sigma	Fit Index	Inten. Corrn.	Std. Corrn.	Element %	Sigma %	Atomic %		Compound %	Nos. of ions
Mg	K	ED	0.76	0.05	0.03	0.00	0.92	0.68	1.00	1.12	0.07	1.15	MgO	1.86	0.23
Al	K	ED	8.64	0.09	0.45	0.00	0.63	0.78	1.00	11.01	0.11	10.21	Al2O3	20.80	2.04
Si	K	ED	15.66	0.12	0.56	0.00	0.17	0.94	1.00	16.74	0.13	14.91	SiO2	35.82	2.98
Ca	K	ED	0.91	0.05	0.04	0.00	0.13	0.96	1.00	0.94	0.05	0.59	CaO	1.32	0.12
Mn	K	ED	5.24	0.14	0.16	0.00	0.42	0.99	1.00	5.30	0.14	2.41	MnO	6.84	0.48
Fe	K	ED	22.97	0.27	0.44	0.01	0.25	0.96	1.00	23.95	0.28	10.72	FeO	30.81	2.14
O	Ka	ED								38.38	0.25	60.01			12.00
			Cation sum 0.00												

* = <2 Sigma															
Grt 2.2	core	SCH-15													
Elmt	Line	Spectrum	Apparent conc.	Stat. Sigma	k Ratio	k Ratio Sigma	Fit Index	Inten. Corrn.	Std. Corrn.	Element %	Sigma %	Atomic %		Compound %	Nos. of ions
Mg	K	ED	1.20	0.05	0.05	0.00	1.45	0.69	1.00	1.75	0.07	1.79	MgO	2.90	0.36
Al	K	ED	8.55	0.09	0.45	0.00	1.88	0.78	1.00	10.95	0.11	10.06	Al2O3	20.69	2.01
Si	K	ED	15.78	0.12	0.57	0.00	0.48	0.93	1.00	16.92	0.13	14.94	SiO2	36.19	2.99
Ca	K	ED	0.84	0.05	0.04	0.00	0.51	0.96	1.00	0.88	0.05	0.54	CaO	1.23	0.11
Mn	K	ED	3.63	0.12	0.11	0.00	0.82	0.99	1.00	3.68	0.13	1.66	MnO	4.75	0.33
Fe	K	ED	23.76	0.27	0.45	0.01	0.24	0.96	1.00	24.81	0.29	11.02	FeO	31.92	2.20
O	Ka	ED								38.70	0.25	59.99			12.00
			Cation sum 0.00												
* = <2 Sigma															
Grt 3.1	core	SMB-10													
Elmt	Line	Spectrum	Apparent conc.	Stat. Sigma	k Ratio	k Ratio Sigma	Fit Index	Inten. Corrn.	Std. Corrn.	Element %	Sigma %	Atomic %		Compound %	Nos. of ions
Mg	K	ED	1.99	0.06	0.08	0.00	0.11	0.70	1.00	2.85	0.08	2.80	MgO	4.72	0.56
Al	K	ED	8.92	0.09	0.47	0.00	0.15	0.78	1.00	11.43	0.12	10.12	Al2O3	21.60	2.02
Si	K	ED	16.30	0.12	0.58	0.00	0.41	0.93	1.00	17.58	0.13	14.95	SiO2	37.60	2.99
Ca	K	ED	0.99	0.05	0.05	0.00	0.90	0.95	1.00	1.04	0.06	0.62	CaO	1.45	0.12
Mn	K	ED	0.81	0.09	0.02	0.00	0.10	0.98	1.00	0.83	0.09	0.36	MnO	1.07	0.07
Fe	K	ED	24.83	0.27	0.47	0.01	0.41	0.95	1.00	26.05	0.29	11.14	FeO	33.51	2.23
O	Ka	ED								40.18	0.25	60.01			12.00
			Cation sum 0.00												
* = <2 Sigma															
Grt 3.2	rim	SMB-10													
Elmt	Line	Spectrum	Apparent conc.	Stat. Sigma	k Ratio	k Ratio Sigma	Fit Index	Inten. Corrn.	Std. Corrn.	Element %	Sigma %	Atomic %		Compound %	Nos. of ions
Mg	K	ED	1.14	0.05	0.05	0.00	0.19	0.69	1.00	1.67	0.07	1.67	MgO	2.76	0.33
Al	K	ED	8.79	0.09	0.46	0.00	0.49	0.78	1.00	11.23	0.11	10.16	Al2O3	21.22	2.03
Si	K	ED	15.97	0.12	0.57	0.00	0.89	0.93	1.00	17.12	0.13	14.88	SiO2	36.63	2.98
Ca	K	ED	0.96	0.05	0.04	0.00	0.27	0.96	1.00	1.00	0.06	0.61	CaO	1.40	0.12
Mn	K	ED	3.94	0.13	0.12	0.00	0.26	0.99	1.00	3.99	0.13	1.77	MnO	5.15	0.35
Fe	K	ED	23.90	0.28	0.46	0.01	0.20	0.96	1.00	24.96	0.29	10.91	FeO	32.11	2.18
O	Ka	ED								39.30	0.25	59.98			12.00
			Cation sum 0.00												
* = <2 Sigma															
Grt 4.1	core	PC-3													
Elmt	Line	Spectrum	Apparent conc.	Stat. Sigma	k Ratio	k Ratio Sigma	Fit Index	Inten. Corrn.	Std. Corrn.	Element %	Sigma %	Atomic %		Compound %	Nos. of ions
Mg	K	ED	1.72	0.09	0.07	0.00	0.26	0.70	1.00	2.45	0.13	2.43	MgO	4.07	0.49
Al	K	ED	8.94	0.14	0.47	0.01	0.97	0.79	1.00	11.38	0.18	10.16	Al2O3	21.50	2.03
Si	K	ED	16.49	0.18	0.59	0.01	1.46	0.93	1.00	17.70	0.19	15.18	SiO2	37.86	3.03
Ca	K	ED	0.84	0.07	0.04	0.00	0.26	0.95	1.00	0.88	0.08	0.53	CaO	1.24	0.11
Mn	K	ED	2.23	0.15	0.07	0.00	0.45	0.98	1.00	2.27	0.15	1.00	MnO	2.93	0.20
Fe	K	ED	23.38	0.36	0.45	0.01	0.44	0.95	1.00	24.51	0.38	10.57	FeO	31.53	2.11
O	Ka	ED								39.94	0.37	60.13			12.00
			Cation sum 0.00												
* = <2 Sigma															

Grt 4.2	rim	PC-3														
Elmt	Line	Spectrum	Apparent conc.	Stat. Sigma	k Ratio	k Ratio Sigma	Fit Index	Inten. Corrn.	Std. Corrn.	Element %	Sigma %	Atomic %		Compound %	Nos. of ions	
Mg	K	ED	0.85	0.08	0.04	0.00	0.24	0.69	1.00	1.23	0.12	1.24	MgO	2.04	0.25	
Al	K	ED	9.00	0.14	0.47	0.01	0.22	0.79	1.00	11.36	0.18	10.31	Al2O3	21.47	2.06	
Si	K	ED	16.35	0.18	0.59	0.01	0.99	0.94	1.00	17.43	0.19	15.19	SiO2	37.28	3.03	
Ca	K	ED	0.82	0.08	0.04	0.00	0.26	0.96	1.00	0.86	0.08	0.53	CaO	1.20	0.10	
Mn	K	ED	6.04	0.20	0.18	0.01	0.28	0.99	1.00	6.11	0.20	2.72	MnO	7.89	0.54	
Fe	K	ED	21.48	0.35	0.41	0.01	0.56	0.96	1.00	22.43	0.37	9.83	FeO	28.85	1.96	
O	Ka	ED								39.32	0.37	60.17			12.00	
			Cation sum 0.00													
* = <2 Sigma																
GRT 5.1	core	SCH-13														
Elmt	Line	Spectrum	Apparent conc.	Stat. Sigma	k Ratio	k Ratio Sigma	Fit Index	Inten. Corrn.	Std. Corrn.	Element %	Sigma %	Atomic %		Compound %	Nos. of ions	
Mg	K	ED	1.12	0.05	0.05	0.00	0.16	0.68	1.00	1.65	0.07	1.63	MgO	2.73	0.33	
Al	K	ED	8.99	0.09	0.47	0.00	0.10	0.78	1.00	11.52	0.12	10.26	Al2O3	21.77	2.05	
Si	K	ED	16.26	0.12	0.58	0.00	0.17	0.93	1.00	17.51	0.13	14.98	SiO2	37.45	2.99	
Ca	K	ED	0.74	0.05	0.03	0.00	0.16	0.96	1.00	0.77	0.05	0.46	CaO	1.08	0.09	
Mn	K	ED	1.39	0.10	0.04	0.00	1.39	0.99	1.00	1.41	0.10	0.62	MnO	1.82	0.12	
Fe	K	ED	26.70	0.28	0.51	0.01	1.37	0.96	1.00	27.90	0.30	12.00	FeO	35.89	2.40	
O	Ka	ED								39.99	0.25	60.05			12.00	
			Cation sum 0.00													
* = <2 Sigma																
GRT 5.2	rim	SCH-13														
Elmt	Line	Spectrum	Apparent conc.	Stat. Sigma	k Ratio	k Ratio Sigma	Fit Index	Inten. Corrn.	Std. Corrn.	Element %	Sigma %	Atomic %		Compound %	Nos. of ions	
Mg	K	ED	0.78	0.05	0.03	0.00	0.23	0.68	1.00	1.15	0.07	1.14	MgO	1.90	0.23	
Al	K	ED	8.83	0.09	0.46	0.00	0.31	0.78	1.00	11.29	0.11	10.15	Al2O3	21.34	2.03	
Si	K	ED	16.27	0.12	0.58	0.00	0.11	0.93	1.00	17.43	0.13	15.05	SiO2	37.29	3.01	
Ca	K	ED	0.68	0.05	0.03	0.00	0.82	0.96	1.00	0.71	0.05	0.43	CaO	1.00	0.09	
Mn	K	ED	3.69	0.12	0.11	0.00	0.61	0.99	1.00	3.73	0.13	1.64	MnO	4.81	0.33	
Fe	K	ED	25.46	0.28	0.48	0.01	0.34	0.96	1.00	26.54	0.29	11.52	FeO	34.15	2.30	
O	Ka	ED								39.63	0.25	60.06			12.00	
			Cation sum 0.00													
* = <2 Sigma																
GRT 6.1	core	SCH-13														
Elmt	Line	Spectrum	Apparent conc.	Stat. Sigma	k Ratio	k Ratio Sigma	Fit Index	Inten. Corrn.	Std. Corrn.	Element %	Sigma %	Atomic %		Compound %	Nos. of ions	
Mg	K	ED	1.08	0.05	0.04	0.00	0.68	0.68	1.00	1.57	0.07	1.56	MgO	2.61	0.31	
Al	K	ED	8.98	0.09	0.47	0.00	0.21	0.78	1.00	11.49	0.12	10.27	Al2O3	21.71	2.05	
Si	K	ED	16.31	0.12	0.58	0.00	0.11	0.93	1.00	17.54	0.13	15.07	SiO2	37.53	3.01	
Ca	K	ED	0.66	0.05	0.03	0.00	0.19	0.96	1.00	0.69	0.05	0.42	CaO	0.97	0.08	
Mn	K	ED	1.48	0.09	0.04	0.00	0.35	0.99	1.00	1.50	0.10	0.66	MnO	1.93	0.13	
Fe	K	ED	26.43	0.28	0.50	0.01	0.30	0.96	1.00	27.61	0.30	11.93	FeO	35.52	2.38	
O	Ka	ED								39.86	0.25	60.10			12.00	
			Cation sum 0.00													

* = <2 Sigma															
GRT 6.2	rim	SCH-13													
Elmt	Line	Spectrum	Apparent conc.	Stat. Sigma	k Ratio	k Ratio Sigma	Fit Index	Inten. Corrn.	Std. Corrn.	Element %	Sigma %	Atomic %		Compound %	Nos. of ions
Mg	K	ED	0.56	0.04	0.02	0.00	0.47	0.68	1.00	0.82	0.06	0.82	MgO	1.36	0.16
Al	K	ED	9.00	0.09	0.47	0.00	0.24	0.79	1.00	11.41	0.11	10.32	Al2O3	21.56	2.06
Si	K	ED	16.31	0.12	0.58	0.00	0.08	0.94	1.00	17.40	0.13	15.12	SiO2	37.23	3.02
Ca	K	ED	0.72	0.05	0.03	0.00	0.60	0.96	1.00	0.75	0.05	0.45	CaO	1.04	0.09
Mn	K	ED	5.67	0.14	0.17	0.00	0.59	0.99	1.00	5.73	0.14	2.55	MnO	7.40	0.51
Fe	K	ED	23.25	0.27	0.44	0.01	0.65	0.96	1.00	24.23	0.28	10.59	FeO	31.17	2.11
O	Ka	ED								39.42	0.25	60.14			12.00
			Cation sum 0.00												
* = <2 Sigma															
GRT 7	core	SCH-14													
Elmt	Line	Spectrum	Apparent conc.	Stat. Sigma	k Ratio	k Ratio Sigma	Fit Index	Inten. Corrn.	Std. Corrn.	Element %	Sigma %	Atomic %		Compound %	Nos. of ions
Mg	K	ED	0.95	0.05	0.04	0.00	1.05	0.68	1.00	1.41	0.07	1.45	MgO	2.33	0.29
Al	K	ED	8.45	0.09	0.44	0.00	0.18	0.78	1.00	10.89	0.11	10.08	Al2O3	20.57	2.02
Si	K	ED	15.58	0.12	0.56	0.00	0.00	0.93	1.00	16.77	0.13	14.92	SiO2	35.87	2.99
Ca	K	ED	0.69	0.05	0.03	0.00	0.18	0.96	1.00	0.72	0.05	0.45	CaO	1.00	0.09
Mn	K	ED	1.44	0.10	0.04	0.00	0.24	0.99	1.00	1.45	0.10	0.66	MnO	1.87	0.13
Fe	K	ED	26.69	0.28	0.51	0.01	0.37	0.96	1.00	27.84	0.30	12.46	FeO	35.81	2.49
O	Ka	ED								38.40	0.25	59.98			12.00
			Cation sum 0.00												
* = <2 Sigma															
GRT7	rim	SCH-14													
Elmt	Line	Spectrum	Apparent conc.	Stat. Sigma	k Ratio	k Ratio Sigma	Fit Index	Inten. Corrn.	Std. Corrn.	Element %	Sigma %	Atomic %		Compound %	Nos. of ions
Mg	K	ED	0.79	0.05	0.03	0.00	0.02	0.68	1.00	1.18	0.07	1.20	MgO	1.95	0.24
Al	K	ED	8.52	0.09	0.45	0.00	0.00	0.78	1.00	10.94	0.11	10.09	Al2O3	20.67	2.02
Si	K	ED	15.72	0.12	0.56	0.00	0.06	0.93	1.00	16.88	0.13	14.96	SiO2	36.10	2.99
Ca	K	ED	0.64	0.05	0.03	0.00	0.35	0.96	1.00	0.67	0.05	0.41	CaO	0.93	0.08
Mn	K	ED	3.03	0.12	0.09	0.00	0.77	0.99	1.00	3.06	0.12	1.39	MnO	3.95	0.28
Fe	K	ED	25.73	0.28	0.49	0.01	0.44	0.96	1.00	26.81	0.29	11.95	FeO	34.49	2.39
O	Ka	ED								38.57	0.25	60.00			12.00
			Cation sum 0.00												
* = <2 Sigma															
GRT 8.1	core	SCH-16													
Elmt	Line	Spectrum	Apparent conc.	Stat. Sigma	k Ratio	k Ratio Sigma	Fit Index	Inten. Corrn.	Std. Corrn.	Element %	Sigma %	Atomic %		Compound %	Nos. of ions
Mg	K	ED	1.09	0.05	0.05	0.00	0.50	0.69	1.00	1.59	0.07	1.64	MgO	2.64	0.33
Al	K	ED	8.53	0.09	0.45	0.00	0.22	0.78	1.00	10.89	0.11	10.11	Al2O3	20.58	2.02
Si	K	ED	15.69	0.12	0.56	0.00	0.17	0.93	1.00	16.81	0.13	14.99	SiO2	35.96	3.00
Ca	K	ED	0.88	0.05	0.04	0.00	0.47	0.96	1.00	0.92	0.05	0.57	CaO	1.28	0.11
Mn	K	ED	3.65	0.12	0.11	0.00	0.22	0.99	1.00	3.69	0.12	1.68	MnO	4.77	0.34
Fe	K	ED	23.43	0.27	0.45	0.01	0.90	0.96	1.00	24.47	0.28	10.98	FeO	31.48	2.19
O	Ka	ED								38.34	0.25	60.02			12.00

			Cation sum 0.00												
* = <2 Sigma															
GRT 8.1	core	SCH-16													
Elmt	Line	Spectrum	Apparent conc.	Stat. Sigma	k Ratio	k Ratio Sigma	Fit Index	Inten. Corrn.	Std. Corrn.	Element %	Sigma %	Atomic %		Compound %	Nos. of ions
Mg	K	ED	1.09	0.05	0.05	0.00	0.50	0.69	1.00	1.59	0.07	1.64	MgO	2.64	0.33
Al	K	ED	8.53	0.09	0.45	0.00	0.22	0.78	1.00	10.89	0.11	10.11	Al2O3	20.58	2.02
Si	K	ED	15.69	0.12	0.56	0.00	0.17	0.93	1.00	16.81	0.13	14.99	SiO2	35.96	3.00
Ca	K	ED	0.88	0.05	0.04	0.00	0.47	0.96	1.00	0.92	0.05	0.57	CaO	1.28	0.11
Mn	K	ED	3.65	0.12	0.11	0.00	0.22	0.99	1.00	3.69	0.12	1.68	MnO	4.77	0.34
Fe	K	ED	23.43	0.27	0.45	0.01	0.90	0.96	1.00	24.47	0.28	10.98	FeO	31.48	2.19
O	Ka	ED								38.34	0.25	60.02			12.00
			Cation sum 0.00												
* = <2 Sigma															
GRT 8.2	rim	SCH-16													
Elmt	Line	Spectrum	Apparent conc.	Stat. Sigma	k Ratio	k Ratio Sigma	Fit Index	Inten. Corrn.	Std. Corrn.	Element %	Sigma %	Atomic %		Compound %	Nos. of ions
Mg	K	ED	0.47	0.04	0.02	0.00	0.53	0.68	1.00	0.70	0.06	0.74	MgO	1.16	0.15
Al	K	ED	8.28	0.09	0.43	0.00	0.13	0.79	1.00	10.53	0.11	10.02	Al2O3	19.89	2.00
Si	K	ED	15.55	0.12	0.56	0.00	0.18	0.94	1.00	16.53	0.13	15.11	SiO2	35.36	3.02
Ca	K	ED	0.76	0.05	0.04	0.00	0.35	0.96	1.00	0.79	0.05	0.51	CaO	1.11	0.10
Mn	K	ED	7.22	0.16	0.21	0.00	0.15	0.99	1.00	7.28	0.16	3.40	MnO	9.40	0.68
Fe	K	ED	21.25	0.26	0.40	0.01	0.15	0.96	1.00	22.11	0.27	10.17	FeO	28.45	2.03
O	Ka	ED								37.42	0.25	60.06			12.00
			Cation sum 0.00												
* = <2 Sigma															
GRT 9.1	core	SMB-9													
Elmt	Line	Spectrum	Apparent conc.	Stat. Sigma	k Ratio	k Ratio Sigma	Fit Index	Inten. Corrn.	Std. Corrn.	Element %	Sigma %	Atomic %		Compound %	Nos. of ions
Mg	K	ED	1.05	0.05	0.04	0.00	0.26	0.69	1.00	1.54	0.07	1.52	MgO	2.55	0.30
Al	K	ED	8.97	0.09	0.47	0.00	0.10	0.78	1.00	11.44	0.12	10.21	Al2O3	21.61	2.04
Si	K	ED	16.47	0.12	0.59	0.00	0.35	0.93	1.00	17.65	0.13	15.14	SiO2	37.75	3.02
Ca	K	ED	0.67	0.05	0.03	0.00	0.30	0.96	1.00	0.71	0.05	0.42	CaO	0.99	0.08
Mn	K	ED	3.34	0.12	0.10	0.00	0.79	0.99	1.00	3.38	0.12	1.48	MnO	4.37	0.30
Fe	K	ED	24.60	0.28	0.47	0.01	0.93	0.96	1.00	25.70	0.29	11.09	FeO	33.06	2.21
O	Ka	ED								39.92	0.26	60.12			12.00
			Cation sum 0.00												
* = <2 Sigma															
GRT 9.2	rim	SMB-9													
Elmt	Line	Spectrum	Apparent conc.	Stat. Sigma	k Ratio	k Ratio Sigma	Fit Index	Inten. Corrn.	Std. Corrn.	Element %	Sigma %	Atomic %		Compound %	Nos. of ions
Mg	K	ED	0.92	0.05	0.04	0.00	0.47	0.69	1.00	1.34	0.07	1.34	MgO	2.22	0.27
Al	K	ED	8.90	0.09	0.47	0.00	0.64	0.79	1.00	11.31	0.11	10.24	Al2O3	21.38	2.04
Si	K	ED	16.22	0.12	0.58	0.00	0.10	0.94	1.00	17.34	0.13	15.08	SiO2	37.10	3.01
Ca	K	ED	0.71	0.05	0.03	0.00	0.14	0.96	1.00	0.74	0.05	0.45	CaO	1.03	0.09
Mn	K	ED	4.90	0.14	0.15	0.00	0.21	0.99	1.00	4.96	0.14	2.20	MnO	6.40	0.44
Fe	K	ED	23.20	0.27	0.44	0.01	0.13	0.96	1.00	24.21	0.29	10.59	FeO	31.15	2.11

O	Ka	ED								39.38	0.25	60.10			12.00
			Cation sum 0.00												
* = <2 Sigma															
10 Garnet Core		SCH-26													
Elmt	Line	Spectrum	Apparent conc.	Stat. Sigma	k Ratio	k Ratio Sigma	Fit Index	Inten. Corrn.	Std. Corrn.	Element %	Sigma %	Atomic %		Compound %	Nos. of ions
Mg	K	ED	1.40	0.05	0.06	0.00	0.27	0.69	1.00	2.03	0.07	2.10	MgO	3.37	0.42
Al	K	ED	8.50	0.09	0.45	0.00	0.93	0.78	1.00	10.89	0.11	10.15	Al2O3	20.58	2.03
Si	K	ED	15.60	0.12	0.56	0.00	1.59	0.93	1.00	16.78	0.13	15.03	SiO2	35.90	3.00
Ca	K	ED	0.78	0.05	0.05	0.00	0.29	1.04	1.00	0.75	0.05	0.47	CaO	1.06	0.09
Mn	K	ED	1.63	0.10	0.05	0.00	0.28	0.99	1.00	1.66	0.10	0.76	MnO	2.14	0.15
Fe	K	ED	24.24	0.27	0.46	0.01	0.56	0.96	1.00	25.37	0.28	11.43	FeO	32.64	2.28
O	Ka	ED								38.19	0.25	60.05			12.00
			Cation sum 0.00												
* = <2 Sigma															
10 Garnet Rim		SCH-26													
Elmt	Line	Spectrum	Apparent conc.	Stat. Sigma	k Ratio	k Ratio Sigma	Fit Index	Inten. Corrn.	Std. Corrn.	Element %	Sigma %	Atomic %		Compound %	Nos. of ions
Mg	K	ED	1.35	0.05	0.06	0.00	0.52	0.69	1.00	1.97	0.07	1.93	MgO	3.26	0.39
Al	K	ED	8.98	0.09	0.47	0.00	1.40	0.78	1.00	11.48	0.12	10.16	Al2O3	21.69	2.03
Si	K	ED	16.55	0.12	0.59	0.00	1.65	0.93	1.00	17.78	0.13	15.12	SiO2	38.03	3.02
Ca	K	ED	0.75	0.05	0.05	0.00	0.31	1.04	1.00	0.72	0.05	0.43	CaO	1.01	0.09
Mn	K	ED	2.05	0.11	0.06	0.00	0.20	0.99	1.00	2.08	0.11	0.91	MnO	2.69	0.18
Fe	K	ED	25.35	0.28	0.48	0.01	0.35	0.96	1.00	26.51	0.30	11.34	FeO	34.11	2.26
O	Ka	ED								40.25	0.26	60.10			12.00
			Cation sum 0.00												
* = <2 Sigma															
Garnet Core 11		SCH-22													
Elmt	Line	Spectrum	Apparent conc.	Stat. Sigma	k Ratio	k Ratio Sigma	Fit Index	Inten. Corrn.	Std. Corrn.	Element %	Sigma %	Atomic %		Compound %	Nos. of ions
Mg	K	ED	1.58	0.05	0.07	0.00	0.15	0.69	1.00	2.28	0.08	2.25	MgO	3.78	0.45
Al	K	ED	9.10	0.09	0.48	0.00	0.04	0.78	1.00	11.61	0.12	10.33	Al2O3	21.94	2.07
Si	K	ED	16.12	0.12	0.58	0.00	0.08	0.93	1.00	17.35	0.13	14.83	SiO2	37.12	2.97
Ca	K	ED	0.98	0.06	0.07	0.00	0.22	1.04	1.00	0.95	0.05	0.57	CaO	1.33	0.11
Mn	K	ED	3.14	0.12	0.09	0.00	0.14	0.99	1.00	3.19	0.12	1.39	MnO	4.12	0.28
Fe	K	ED	23.63	0.28	0.45	0.01	0.23	0.96	1.00	24.73	0.29	10.63	FeO	31.82	2.13
O	Ka	ED								39.99	0.26	60.00			12.00
			Cation sum 0.00												
* = <2 Sigma															
Garnet Rim 11		SCH-22													
Elmt	Line	Spectrum	Apparent conc.	Stat. Sigma	k Ratio	k Ratio Sigma	Fit Index	Inten. Corrn.	Std. Corrn.	Element %	Sigma %	Atomic %		Compound %	Nos. of ions
Mg	K	ED	0.92	0.05	0.04	0.00	0.00	0.69	1.00	1.34	0.07	1.32	MgO	2.23	0.26
Al	K	ED	9.10	0.09	0.48	0.00	0.24	0.79	1.00	11.54	0.12	10.25	Al2O3	21.81	2.04
Si	K	ED	16.65	0.13	0.60	0.00	0.24	0.94	1.00	17.78	0.13	15.17	SiO2	38.04	3.03
Ca	K	ED	0.93	0.06	0.06	0.00	0.53	1.04	1.00	0.90	0.05	0.54	CaO	1.25	0.11
Mn	K	ED	4.92	0.14	0.15	0.00	1.50	0.99	1.00	4.98	0.14	2.17	MnO	6.43	0.43

Fe	K	ED	23.22	0.28	0.44	0.01	1.16	0.96	1.00	24.25	0.29	10.41	FeO	31.20	2.08
O	Ka	ED								40.16	0.26	60.15			12.00
			Cation sum 0.00												
Garnet 12 Core	PC-2														
Elmt	Line	Spectrum	Apparent conc.	Stat. Sigma	k Ratio	k Ratio Sigma	Fit Index	Inten. Corrn.	Std. Corrn.	Element %	Sigma %	Atomic %		Compound %	Nos. of ions
Mg	K	ED	1.61	0.05	0.07	0.00	1.37	0.69	1.00	2.34	0.08	2.42	MgO	3.88	0.48
Al	K	ED	8.42	0.09	0.44	0.00	0.57	0.78	1.00	10.83	0.11	10.08	Al2O3	20.46	2.02
Si	K	ED	15.49	0.12	0.55	0.00	0.59	0.93	1.00	16.69	0.13	14.93	SiO2	35.71	2.99
Ca	K	ED	0.73	0.05	0.05	0.00	0.30	1.04	1.00	0.70	0.05	0.44	CaO	0.98	0.09
Mn	K	ED	1.63	0.10	0.05	0.00	0.21	0.99	1.00	1.65	0.10	0.75	MnO	2.13	0.15
Fe	K	ED	24.19	0.28	0.46	0.01	0.32	0.96	1.00	25.32	0.29	11.39	FeO	32.57	2.28
O	Ka	ED								38.20	0.25	59.99			12.00
			Cation sum 0.00												
* = <2 Sigma															
Garnet 12 Rim	PC-2														
Elmt	Line	Spectrum	Apparent conc.	Stat. Sigma	k Ratio	k Ratio Sigma	Fit Index	Inten. Corrn.	Std. Corrn.	Element %	Sigma %	Atomic %		Compound %	Nos. of ions
Mg	K	ED	1.06	0.05	0.04	0.00	0.23	0.68	1.00	1.56	0.07	1.63	MgO	2.59	0.33
Al	K	ED	8.29	0.09	0.43	0.00	0.21	0.78	1.00	10.65	0.11	9.99	Al2O3	20.13	2.00
Si	K	ED	15.36	0.12	0.55	0.00	0.97	0.93	1.00	16.47	0.13	14.84	SiO2	35.24	2.97
Ca	K	ED	0.61	0.05	0.04	0.00	0.04	1.04	1.00	0.58	0.05	0.37	CaO	0.81	0.07
Mn	K	ED	5.04	0.14	0.15	0.00	0.32	0.99	1.00	5.09	0.14	2.34	MnO	6.57	0.47
Fe	K	ED	23.11	0.27	0.44	0.01	0.12	0.96	1.00	24.08	0.29	10.91	FeO	30.97	2.19
O	Ka	ED								37.88	0.25	59.92			12.00
			Cation sum 0.00												
* = <2 Sigma															
GRT 13	core	SCH-3													
Elmt	Line	Spectrum	Apparent conc.	Stat. Sigma	k Ratio	k Ratio Sigma	Fit Index	Inten. Corrn.	Std. Corrn.	Element %	Sigma %	Atomic %		Compound %	Nos. of ions
Mg	K	ED	2.29	0.06	0.10	0.00	0.76	0.71	1.00	3.23	0.08	3.14	MgO	5.36	0.63
Al	K	ED	9.14	0.09	0.48	0.00	1.04	0.79	1.00	11.64	0.12	10.17	Al2O3	21.98	2.03
Si	K	ED	16.78	0.13	0.60	0.00	0.27	0.93	1.00	18.04	0.13	15.15	SiO2	38.60	3.02
Ca	K	ED	1.05	0.06	0.07	0.00	0.34	1.03	1.00	1.01	0.06	0.60	CaO	1.42	0.12
Mn	K	ED	1.52	0.10	0.05	0.00	0.31	0.98	1.00	1.55	0.10	0.66	MnO	2.00	0.13
Fe	K	ED	22.92	0.27	0.44	0.01	0.72	0.95	1.00	24.10	0.28	10.17	FeO	31.00	2.03
O	Ka	ED								40.79	0.26	60.11			12.00
			Cation sum 0.00												
* = <2 Sigma															
GRT 13 RIM		SCH-3													
Elmt	Line	Spectrum	Apparent conc.	Stat. Sigma	k Ratio	k Ratio Sigma	Fit Index	Inten. Corrn.	Std. Corrn.	Element %	Sigma %	Atomic %		Compound %	Nos. of ions
Mg	K	ED	0.80	0.05	0.03	0.00	0.32	0.68	1.00	1.17	0.07	1.17	MgO	1.94	0.23
Al	K	ED	8.86	0.09	0.46	0.00	0.30	0.79	1.00	11.28	0.12	10.16	Al2O3	21.31	2.03
Si	K	ED	16.30	0.12	0.58	0.00	0.51	0.94	1.00	17.41	0.13	15.06	SiO2	37.24	3.01
Ca	K	ED	1.00	0.06	0.07	0.00	0.26	1.04	1.00	0.96	0.06	0.58	CaO	1.35	0.12

Mn	K	ED	4.88	0.14	0.15	0.00	0.81	0.99	1.00	4.93	0.14	2.18	MnO	6.37	0.44
Fe	K	ED	23.76	0.28	0.45	0.01	0.97	0.96	1.00	24.79	0.29	10.78	FeO	31.89	2.15
O	Ka	ED								39.56	0.26	60.07			12.00
			Cation sum 0.00												
* = <2 Sigma															
Grt 14	core	SMB-15													
Elmt	Line	Spectrum	Apparent conc.	Stat. Sigma	k Ratio	k Ratio Sigma	Fit Index	Inten. Corrn.	Std. Corrn.	Element %	Sigma %	Atomic %		Compound %	Nos. of ions
Mg	K	ED	1.17	0.05	0.05	0.00	0.42	0.69	1.00	1.71	0.07	1.70	MgO	2.84	0.34
Al	K	ED	8.88	0.09	0.47	0.00	0.31	0.78	1.00	11.35	0.12	10.13	Al2O3	21.45	2.02
Si	K	ED	16.37	0.12	0.59	0.00	0.32	0.93	1.00	17.56	0.13	15.06	SiO2	37.57	3.01
Ca	K	ED	0.74	0.05	0.05	0.00	0.29	1.04	1.00	0.71	0.05	0.43	CaO	1.00	0.09
Mn	K	ED	3.23	0.12	0.10	0.00	0.47	0.99	1.00	3.27	0.12	1.43	MnO	4.22	0.29
Fe	K	ED	24.85	0.28	0.47	0.01	0.27	0.96	1.00	25.96	0.29	11.19	FeO	33.40	2.24
O	Ka	ED								39.91	0.26	60.06			12.00
			Cation sum 0.00												
* = <2 Sigma															
Grt 14	rim	SMB-15													
Elmt	Line	Spectrum	Apparent conc.	Stat. Sigma	k Ratio	k Ratio Sigma	Fit Index	Inten. Corrn.	Std. Corrn.	Element %	Sigma %	Atomic %		Compound %	Nos. of ions
Mg	K	ED	0.72	0.05	0.03	0.00	0.50	0.68	1.00	1.07	0.07	1.06	MgO	1.77	0.21
Al	K	ED	8.82	0.09	0.46	0.00	0.70	0.78	1.00	11.28	0.12	10.05	Al2O3	21.31	2.01
Si	K	ED	16.60	0.13	0.59	0.00	1.00	0.93	1.00	17.76	0.13	15.21	SiO2	38.00	3.04
Ca	K	ED	0.66	0.05	0.05	0.00	0.18	1.04	1.00	0.64	0.05	0.38	CaO	0.89	0.08
Mn	K	ED	3.24	0.12	0.10	0.00	0.49	0.99	1.00	3.28	0.12	1.44	MnO	4.23	0.29
Fe	K	ED	26.17	0.29	0.50	0.01	0.40	0.96	1.00	27.28	0.30	11.75	FeO	35.10	2.35
O	Ka	ED								40.00	0.26	60.12			12.00
			Cation sum 0.00												
* = <2 Sigma															

800.00 rim																
Elmt	Line	Spectrum	Apparent conc.	Stat. Sigma	k Ratio	k Ratio Sigma	Fit Index	Inten. Corrn.	Std. Corrn.	Element %	Sigma %	Atomic %		Compound %	Nos. of ions	
Mg	K	ED	1.16	0.05	0.05	0.00	0.00	0.69	1.00	1.69	0.07	1.67	MgO	2.81	0.33	
Al	K	ED	8.49	0.09	0.26	0.00	0.03	0.73	1.00	11.62	0.12	10.32	Al2O3	21.96	2.06	
Si	K	ED	16.28	0.12	0.58	0.00	0.04	0.93	1.00	17.50	0.13	14.93	SiO2	37.45	2.98	
Ca	K	ED	0.70	0.05	0.03	0.00	0.45	0.96	1.00	0.73	0.05	0.44	CaO	1.02	0.09	
Mn	K	ED	2.99	0.12	0.09	0.00	0.84	0.99	1.00	3.03	0.12	1.32	MnO	3.91	0.26	
Fe	K	ED	25.14	0.28	0.48	0.01	1.17	0.96	1.00	26.26	0.29	11.27	FeO	33.78	2.25	
O	Ka	ED								40.09	0.26	60.05			12.00	
			Cation sum 0.00													
* = <2 Sigma																
800.00 rim																
Elmt	Line	Spectrum	Apparent conc.	Stat. Sigma	k Ratio	k Ratio Sigma	Fit Index	Inten. Corrn.	Std. Corrn.	Element %	Sigma %	Atomic %		Compound %	Nos. of ions	
Mg	K	ED	3.79	0.07	0.16	0.00	0.19	0.74	1.00	5.11	0.09	4.77	MgO	8.48	0.95	
Al	K	ED	9.01	0.09	0.27	0.00	0.39	0.74	1.00	12.20	0.12	10.27	Al2O3	23.05	2.05	
Si	K	ED	17.25	0.13	0.62	0.00	0.44	0.93	1.00	18.57	0.14	15.01	SiO2	39.73	3.00	
Ca	K	ED	1.40	0.06	0.06	0.00	0.18	0.94	1.00	1.49	0.06	0.84	CaO	2.08	0.17	
Mn	K	ED	2.34	0.11	0.07	0.00	0.86	0.97	1.00	2.40	0.11	0.99	MnO	3.10	0.20	
Fe	K	ED	18.70	0.25	0.36	0.00	1.22	0.94	1.00	19.79	0.26	8.05	FeO	25.46	1.61	
O	Ka	ED								42.33	0.25	60.07			12.00	
			Cation sum 0.00													
* = <2 Sigma																
800.00 opx																
Elmt	Line	Spectrum	Apparent conc.	Stat. Sigma	k Ratio	k Ratio Sigma	Fit Index	Inten. Corrn.	Std. Corrn.	Element %	Sigma %	Atomic %		Compound %	Nos. of ions	
Mg	K	ED	4.82	0.07	0.20	0.00	0.03	0.69	1.00	7.02	0.10	6.98	MgO	11.64	0.70	
Al	K	ED	0.28	0.05	0.01	0.00	0.15	0.68	1.00	0.41	0.07	0.37	Al2O3	0.78	0.04	
Si	K	ED	23.60	0.14	0.85	0.00	0.80	1.01	1.00	23.46	0.14	20.19	SiO2	50.19	2.01	
Ca	K	ED	0.30	0.05	0.01	0.00	0.35	0.95	1.00	0.31	0.05	0.19	CaO	0.44	0.02	
Mn	K	ED	1.65	0.10	0.05	0.00	0.22	0.98	1.00	1.68	0.10	0.74	MnO	2.16	0.07	
Fe	K	ED	25.00	0.28	0.48	0.01	0.57	0.95	1.00	26.24	0.29	11.35	FeO	33.76	1.13	
O	Ka	ED								39.85	0.24	60.19			6.00	
			Cation sum 0.00													
* = <2 Sigma																
800.00 glass																
Elmt	Line	Spectrum	Apparent conc.	Stat. Sigma	k Ratio	k Ratio Sigma	Fit Index	Inten. Corrn.	Std. Corrn.	Element %	Sigma %	Atomic %		Compound %	Nos. of ions	
Na	K	ED	2.02	0.07	0.18	0.01	0.02	0.90	1.00	2.24	0.07	2.39	Na2O	3.01	0.38	
Mg	K	ED	0.11	0.04	0.00	0.00	0.26	0.89	1.00	0.12	0.05	0.13	MgO	0.21	0.02	
Al	K	ED	6.80	0.08	0.20	0.00	0.42	0.92	1.00	7.39	0.09	6.74	Al2O3	13.96	1.07	
Si	K	ED	31.65	0.16	1.13	0.01	0.37	1.12	1.00	28.31	0.14	24.80	SiO2	60.57	3.92	

K	K	ED	1.86	0.06	0.15	0.00	0.36	0.98	1.00	1.89	0.06	1.19	K2O	2.28	0.19	
Ca	K	ED	1.29	0.05	0.06	0.00	0.37	0.89	1.00	1.46	0.06	0.90	CaO	2.04	0.14	
Ti	K	ED	0.07	0.04	0.00	0.00	0.12	0.86	1.00	0.08	0.05	0.04	TiO2	0.13	0.01	
Mn	K	ED	0.17	0.06	0.01	0.00	0.11	0.94	1.00	0.19	0.06	0.08	MnO	0.24	0.01	
Fe	K	ED	1.08	0.09	0.02	0.00	0.16	0.91	1.00	1.19	0.10	0.52	FeO	1.53	0.08	
O	Ka	ED								41.11	0.20	63.21			10.00	
			Cation sum 0.00													
* = <2 Sigma																
800.00	glass															
Elmt	Line	Spectrum	Apparent conc.	Stat. Sigma	k Ratio	k Ratio Sigma	Fit Index	Inten. Corrn.	Std. Corrn.	Element %	Sigma %	Atomic %		Compound %	Nos. of ions	
Na	K	ED	2.09	0.07	0.19	0.01	0.00	0.90	1.00	2.32	0.07	2.19	Na2O	3.13	0.35	
Mg	K	ED	0.06	0.05	0.00	0.00	0.08	0.89	1.00	0.07	0.05	0.06	MgO	0.11	0.01	
Al	K	ED	7.73	0.08	0.23	0.00	0.78	0.92	1.00	8.37	0.09	6.74	Al2O3	15.81	1.06	
Si	K	ED	36.21	0.17	1.30	0.01	2.03	1.12	1.00	32.31	0.15	24.98	SiO2	69.12	3.95	
K	K	ED	2.12	0.06	0.17	0.01	0.17	0.98	1.00	2.16	0.06	1.20	K2O	2.61	0.19	
Ca	K	ED	1.53	0.06	0.07	0.00	0.39	0.89	1.00	1.73	0.06	0.94	CaO	2.42	0.15	
Ti	K	ED	-0.04	0.04	0.00	0.00	0.23	0.86	1.00	-0.05	0.05	-0.02	TiO2	-0.08	0.00	
Mn	K	ED	0.03	0.06	0.00	0.00	0.24	0.94	1.00	0.03	0.07	0.01	MnO	0.04	0.00	
Fe	K	ED	1.38	0.09	0.03	0.00	0.37	0.91	1.00	1.51	0.10	0.59	FeO	1.94	0.09	
O	Ka	ED								46.65	0.21	63.32			10.00	
			Cation sum 0.00													
* = <2 Sigma																
800.00	gkass with crystals															
Elmt	Line	Spectrum	Apparent conc.	Stat. Sigma	k Ratio	k Ratio Sigma	Fit Index	Inten. Corrn.	Std. Corrn.	Element %	Sigma %	Atomic %		Compound %	Nos. of ions	
Na	K	ED	2.15	0.07	0.19	0.01	0.20	0.88	1.00	2.45	0.08	2.32	Na2O	3.30	0.37	
Mg	K	ED	0.60	0.05	0.03	0.00	0.23	0.87	1.00	0.70	0.06	0.62	MgO	1.15	0.10	
Al	K	ED	7.29	0.08	0.22	0.00	0.69	0.90	1.00	8.13	0.09	6.57	Al2O3	15.37	1.05	
Si	K	ED	34.29	0.17	1.23	0.01	1.17	1.10	1.00	31.09	0.15	24.13	SiO2	66.50	3.84	
K	K	ED	2.30	0.06	0.19	0.01	0.31	0.99	1.00	2.33	0.07	1.30	K2O	2.81	0.21	
Ca	K	ED	1.30	0.05	0.06	0.00	0.29	0.89	1.00	1.46	0.06	0.79	CaO	2.04	0.13	
Ti	K	ED	0.25	0.05	0.00	0.00	0.99	0.86	1.00	0.29	0.06	0.13	TiO2	0.49	0.02	
Mn	K	ED	0.17	0.06	0.00	0.00	0.33	0.94	1.00	0.18	0.07	0.07	MnO	0.23	0.01	
Fe	K	ED	2.78	0.12	0.05	0.00	0.14	0.91	1.00	3.04	0.13	1.19	FeO	3.91	0.19	
O	Ka	ED								46.13	0.22	62.87			10.00	
			Cation sum 0.00													
* = <2 Sigma																
700.00	garnet core															
Elmt	Line	Spectrum	Apparent conc.	Stat. Sigma	k Ratio	k Ratio Sigma	Fit Index	Inten. Corrn.	Std. Corrn.	Element %	Sigma %	Atomic %		Compound %	Nos. of ions	
Mg	K	ED	1.15	0.05	0.05	0.00	0.10	0.69	1.00	1.68	0.07	1.67	MgO	2.79	0.33	
Al	K	ED	8.95	0.09	0.47	0.00	0.00	0.78	1.00	11.45	0.12	10.25	Al2O3	21.63	2.05	

Si	K	ED	15.27	0.11	0.48	0.00	0.17	0.88	1.00	17.40	0.13	14.98	SiO2	37.23	2.99
Ca	K	ED	0.69	0.05	0.03	0.00	0.20	0.96	1.00	0.72	0.05	0.44	CaO	1.01	0.09
Mn	K	ED	2.92	0.12	0.09	0.00	0.73	0.99	1.00	2.96	0.12	1.30	MnO	3.82	0.26
Fe	K	ED	25.01	0.28	0.48	0.01	0.57	0.96	1.00	26.12	0.29	11.31	FeO	33.61	2.26
O	Ka	ED								39.75	0.25	60.05			12.00
			Cation sum 0.00												
* = <2 Sigma															
700.00	garnet core near hole														
Elmt	Line	Spectrum	Apparent conc.	Stat. Sigma	k Ratio	k Ratio Sigma	Fit Index	Inten. Corrn.	Std. Corrn.	Element %	Sigma %	Atomic %		Compound %	Nos. of ions
Mg	K	ED	1.15	0.05	0.05	0.00	0.18	0.68	1.00	1.69	0.07	1.72	MgO	2.81	0.35
Al	K	ED	9.17	0.09	0.48	0.00	0.27	0.78	1.00	11.80	0.12	10.83	Al2O3	22.30	2.17
Si	K	ED	13.92	0.11	0.44	0.00	0.39	0.87	1.00	16.05	0.13	14.14	SiO2	34.33	2.84
Ca	K	ED	0.95	0.05	0.04	0.00	0.92	0.96	1.00	0.99	0.06	0.61	CaO	1.38	0.12
Mn	K	ED	1.97	0.10	0.06	0.00	0.11	0.99	1.00	1.99	0.10	0.90	MnO	2.57	0.18
Fe	K	ED	26.00	0.28	0.50	0.01	0.18	0.96	1.00	27.13	0.29	12.02	FeO	34.91	2.41
O	Ka	ED								38.65	0.25	59.78			12.00
			Cation sum 0.00												
* = <2 Sigma															
700.00	rim														
Elmt	Line	Spectrum	Apparent conc.	Stat. Sigma	k Ratio	k Ratio Sigma	Fit Index	Inten. Corrn.	Std. Corrn.	Element %	Sigma %	Atomic %		Compound %	Nos. of ions
Mg	K	ED	1.03	0.05	0.04	0.00	0.00	0.69	1.00	1.50	0.07	1.50	MgO	2.49	0.30
Al	K	ED	8.88	0.09	0.47	0.00	0.04	0.78	1.00	11.33	0.11	10.24	Al2O3	21.40	2.04
Si	K	ED	15.31	0.11	0.48	0.00	0.10	0.88	1.00	17.43	0.13	15.13	SiO2	37.28	3.02
Ca	K	ED	0.63	0.05	0.03	0.00	0.51	0.96	1.00	0.66	0.05	0.40	CaO	0.92	0.08
Mn	K	ED	2.72	0.11	0.08	0.00	0.18	0.99	1.00	2.75	0.11	1.22	MnO	3.55	0.24
Fe	K	ED	24.96	0.27	0.48	0.01	0.20	0.96	1.00	26.07	0.29	11.39	FeO	33.54	2.27
O	Ka	ED								39.45	0.25	60.12			12.00
			Cation sum 0.00												
* = <2 Sigma															
700.00	rim														
Elmt	Line	Spectrum	Apparent conc.	Stat. Sigma	k Ratio	k Ratio Sigma	Fit Index	Inten. Corrn.	Std. Corrn.	Element %	Sigma %	Atomic %		Compound %	Nos. of ions
Mg	K	ED	1.12	0.05	0.05	0.00	0.40	0.68	1.00	1.65	0.07	1.70	MgO	2.74	0.34
Al	K	ED	8.49	0.09	0.45	0.00	0.10	0.78	1.00	10.95	0.11	10.14	Al2O3	20.69	2.03
Si	K	ED	14.56	0.11	0.46	0.00	0.69	0.87	1.00	16.65	0.13	14.82	SiO2	35.63	2.97
Ca	K	ED	0.61	0.05	0.03	0.00	0.27	0.96	1.00	0.64	0.05	0.40	CaO	0.89	0.08
Mn	K	ED	1.70	0.10	0.05	0.00	1.31	0.99	1.00	1.72	0.10	0.78	MnO	2.22	0.16
Fe	K	ED	26.15	0.28	0.50	0.01	1.00	0.96	1.00	27.29	0.29	12.21	FeO	35.10	2.44
O	Ka	ED								38.38	0.25	59.95			12.00
			Cation sum 0.00												

* = <2 Sigma																
700.00	plag															
Elmt	Line	Spectrum	Apparent conc.	Stat. Sigma	k Ratio	k Ratio Sigma	Fit Index	Inten. Corrn.	Std. Corrn.	Element %	Sigma %	Atomic %		Compound %	Nos. of ions	
Na	K	ED	4.91	0.09	0.56	0.01	0.29	0.96	1.00	5.13	0.09	4.55	Na2O	6.91	0.59	
Al	K	ED	13.55	0.11	0.71	0.01	0.30	0.98	1.00	13.90	0.11	10.50	Al2O3	26.26	1.36	
Si	K	ED	27.52	0.15	0.87	0.00	1.48	0.98	1.00	28.16	0.15	20.44	SiO2	60.24	2.65	
K	K	ED	0.40	0.05	0.03	0.00	0.26	0.99	1.00	0.41	0.05	0.21	K2O	0.49	0.03	
Ca	K	ED	5.07	0.08	0.35	0.01	0.33	0.98	1.00	5.18	0.09	2.64	CaO	7.25	0.34	
O	Ka	ED								48.38	0.21	61.66			8.00	
			Cation sum 0.00													
* = <2 Sigma																
700.00	rim															
Elmt	Line	Spectrum	Apparent conc.	Stat. Sigma	k Ratio	k Ratio Sigma	Fit Index	Inten. Corrn.	Std. Corrn.	Element %	Sigma %	Atomic %		Compound %	Nos. of ions	
Mg	K	ED	1.21	0.05	0.05	0.00	0.37	0.69	1.00	1.76	0.07	1.74	MgO	2.92	0.29	
Al	K	ED	9.02	0.09	0.47	0.00	0.19	0.78	1.00	11.50	0.12	10.25	Al2O3	21.73	1.70	
Si	K	ED	15.51	0.12	0.49	0.00	0.01	0.88	1.00	17.66	0.13	15.12	SiO2	37.78	2.51	
Ca	K	ED	0.68	0.05	0.05	0.00	0.69	1.04	1.00	0.66	0.05	0.40	CaO	0.92	0.07	
Mn	K	ED	2.80	0.11	0.08	0.00	0.60	0.99	1.00	2.84	0.11	1.24	MnO	3.66	0.21	
Fe	K	ED	24.73	0.28	0.47	0.01	0.46	0.96	1.00	25.85	0.29	11.13	FeO	33.26	1.85	
O	Ka	ED								40.01	0.25	60.12			10.00	
			Cation sum 0.00													
* = <2 Sigma																
700.00	core															
Elmt	Line	Spectrum	Apparent conc.	Stat. Sigma	k Ratio	k Ratio Sigma	Fit Index	Inten. Corrn.	Std. Corrn.	Element %	Sigma %	Atomic %		Compound %	Nos. of ions	
Mg	K	ED	1.11	0.05	0.05	0.00	0.18	0.69	1.00	1.62	0.07	1.61	MgO	2.69	0.27	
Al	K	ED	8.93	0.09	0.47	0.00	0.13	0.78	1.00	11.39	0.11	10.21	Al2O3	21.53	1.70	
Si	K	ED	15.39	0.11	0.49	0.00	0.24	0.88	1.00	17.52	0.13	15.08	SiO2	37.48	2.51	
Ca	K	ED	0.77	0.05	0.05	0.00	0.41	1.04	1.00	0.74	0.05	0.45	CaO	1.03	0.07	
Mn	K	ED	3.06	0.11	0.09	0.00	0.36	0.99	1.00	3.10	0.12	1.37	MnO	4.01	0.23	
Fe	K	ED	24.76	0.28	0.47	0.01	1.22	0.96	1.00	25.87	0.29	11.20	FeO	33.28	1.86	
O	Ka	ED								39.77	0.25	60.09			10.00	
			Cation sum 0.00													
* = <2 Sigma																

	MUM 06 BM-01	MUM 06 BM-02	MUM 06 BM-03	MUM 06 BM-04	MUM 06 BM-05	MUM 06 BM-06	MUM 06 BM-07	MUM 06 BM-08	MUM 06 BM-10	MUM 06 BM-11	MUM 06 BM-12	MUM 06 BM-13		MUM 06 BM-02	MUM 06 BM-02R	
Date	16-Jan-11	16-Jan-11	16-Jan-11	16-Jan-11	16-Jan-11	16-Jan-11	16-Jan-11	16-Jan-11	16-Jan-11	16-Jan-11	16-Jan-11	16-Jan-11		16-Jan-11	16-Jan-11	
	Unnormalized Major Elements (Weight %):										**Unnormalized Major Elements (Weight %):**					
SiO2	65.07	69.05	63.91	65.41	47.83	70.81	51.30	69.09	65.98	66.24	50.63	66.70		69.05	69.05	
TiO2	0.786	0.481	0.780	0.758	1.264	0.322	1.048	0.465	0.801	0.674	2.653	0.782		0.481	0.480	
Al2O3	16.89	14.89	15.48	16.42	26.61	15.01	23.54	15.25	14.97	16.56	16.10	15.00		14.89	14.90	
FeO*	4.99	3.20	5.10	4.12	8.57	1.94	9.53	2.94	5.17	4.22	11.29	4.64		3.20	3.24	
MnO	0.110	0.077	0.114	0.073	0.239	0.041	0.474	0.048	0.106	0.133	0.209	0.085		0.077	0.077	
MgO	1.92	0.91	1.57	1.73	2.48	0.81	2.70	0.91	1.39	1.20	6.24	1.37		0.91	0.90	
CaO	1.12	1.51	1.98	3.26	0.21	1.37	0.57	1.85	2.50	1.42	9.58	2.12		1.51	1.51	
Na2O	2.65	3.29	3.45	3.87	0.84	3.15	1.36	3.02	3.02	2.41	0.87	3.02		3.29	3.30	
K2O	2.53	4.29	4.11	2.33	5.66	4.65	4.26	3.84	3.21	3.82	0.64	3.91		4.29	4.30	
P2O5	0.190	0.181	0.249	0.258	0.103	0.173	0.090	0.184	0.262	0.195	0.367	0.244		0.181	0.182	
Sum	96.25	97.88	96.74	98.23	93.81	98.28	94.87	97.60	97.41	96.89	98.57	97.88		97.88	97.93	
	Normalized Major Elements (Weight %):										**Normalized Major Elements (Weight %):**					
SiO2	67.60	70.55	66.06	66.59	50.99	72.06	54.08	70.79	67.73	68.37	51.37	68.15		70.55	70.51	
TiO2	0.817	0.491	0.806	0.772	1.347	0.328	1.105	0.476	0.823	0.696	2.692	0.799		0.491	0.490	
Al2O3	17.55	15.21	16.00	16.72	28.37	15.27	24.81	15.62	15.37	17.10	16.33	15.33		15.21	15.21	
FeO*	5.19	3.27	5.27	4.20	9.13	1.97	10.04	3.01	5.31	4.35	11.45	4.74		3.27	3.31	
MnO	0.114	0.079	0.118	0.074	0.254	0.042	0.499	0.049	0.108	0.137	0.213	0.086		0.079	0.079	
MgO	1.99	0.93	1.62	1.76	2.64	0.83	2.85	0.93	1.43	1.23	6.33	1.40		0.93	0.92	
CaO	1.16	1.54	2.05	3.31	0.23	1.39	0.60	1.90	2.56	1.47	9.72	2.17		1.54	1.54	
Na2O	2.76	3.37	3.57	3.94	0.90	3.20	1.44	3.10	3.10	2.49	0.88	3.09		3.37	3.37	
K2O	2.63	4.38	4.25	2.37	6.03	4.73	4.49	3.93	3.29	3.95	0.64	3.99		4.38	4.39	
P2O5	0.197	0.185	0.258	0.263	0.109	0.176	0.095	0.188	0.269	0.202	0.372	0.249		0.185	0.186	
Total	100.00	100.00	100.00	100.00	100.00	100.00	100.00	100.00	100.00	100.00	100.00	100.00		100.00	100.00	
	Unnormalized Trace Elements (ppm):										**Unnormalized Trace Elements (ppm):**					
Ni	18	7	10	4	45	5	66	5	10	15	60	10		7	7	
Cr	47	20	26	20	119	16	129	16	26	40	193	27		20	19	
Sc	11	9	15	13	15	6	14	8	15	15	28	13		9	10	
V	76	41	66	65	134	27	147	33	61	69	270	63		41	43	
Ba	525	570	840	386	1319	489	1335	745	799	739	67	744		570	567	
Rb	97	164	150	139	184	146	118	134	142	154	30	155		164	166	
Sr	139	138	188	212	105	144	242	213	191	173	558	166		138	138	
Zr	274	191	321	169	199	92	163	169	308	220	197	261		191	191	
Y	36	32	47	20	38	14	36	22	42	35	28	32		32	33	
Nb	15.5	10.7	15.2	10.0	26.1	7.8	19.9	9.7	15.2	12.6	41.9	13.1		10.7	9.4	
Ga	24	20	24	20	35	19	29	19	22	22	23	20		20	18	
Cu	22	4	12	2	10	0	0	1	17	15	3	4		4	5	
Zn	116	63	28	85	108	50	130	52	84	76	115	77		63	62	
Pb	9	21	8	11	13	24	20	23	17	21	15	19		21	22	
La	43	27	41	18	84	17	44	34	42	38	27	30		27	28	
Ce	91	56	99	36	162	38	83	72	91	78	58	73		56	58	
Th	14	10	13	5	22	11	11	15	13	13	2	13		10	11	
Nd	45	28	49	22	68	22	37	33	46	38	34	33		28	31	

sum tr.	1603	1412	1953	1236	2685	1126	2621	1601	1940	1773	1750	1753		1412	1417	
in %	0.16	0.14	0.20	0.12	0.27	0.11	0.26	0.16	0.19	0.18	0.17	0.18		0.14	0.14	
sum m+tr	96.41	98.02	96.94	98.35	94.08	98.39	95.13	97.76	97.60	97.06	98.74	98.05		98.02	98.07	
M+Toxides	96.45	98.05	96.98	98.38	94.13	98.41	95.18	97.79	97.64	97.10	98.79	98.09		98.05	98.10	
	Major elements are normalized on a volatile-free basis, with total Fe expressed as FeO.										**Major elements are normalized on a volatile-free basis, with total Fe expressed as FeO.**					
	"R" denotes a duplicate bead made from the same rock powder.										**"R" denotes a duplicate bead made from the same rock powder.**					
NiO	23.2	8.4	13.2	5.3	57.6	7.0	84.4	6.0	12.7	19.7	76.4	12.7		8.4	9.3	
Cr2O3	69.3	28.5	37.6	29.1	173.2	22.7	188.8	23.2	38.3	58.2	282.2	39.8		28.5	27.9	
Sc2O3	16.6	14.1	23.3	19.6	22.7	8.7	20.7	12.1	22.9	22.2	43.3	20.2		14.1	14.9	
V2O3	111.7	60.8	96.7	95.3	196.5	39.3	216.4	48.8	89.0	101.9	397.8	93.3		60.8	63.8	
BaO	585.7	636.2	938.3	430.7	1472.8	546.3	1490.9	832.0	892.3	824.6	74.7	830.2		636.2	633.1	
Rb2O	106.2	179.8	164.1	152.0	201.3	159.1	128.7	146.4	155.1	168.9	32.3	169.7		179.8	181.1	
SrO	164.3	163.3	222.1	250.9	124.6	170.1	286.1	251.3	226.4	204.2	660.2	195.7		163.3	162.7	
ZrO2	374.3	261.2	438.6	230.3	271.3	125.9	221.8	230.7	420.5	299.9	268.8	355.9		261.2	260.8	
Y2O3	45.1	41.0	59.6	25.3	47.9	17.4	45.2	27.4	53.2	45.0	35.6	40.5		41.0	42.2	
Nb2O5	22.2	15.3	21.7	14.3	37.3	11.2	28.5	13.9	21.7	18.0	59.9	18.7		15.3	13.4	
Ga2O3	32.1	27.4	32.7	27.4	47.6	25.4	38.3	26.1	29.3	29.4	31.2	27.4		27.4	24.6	
CuO	27.9	5.4	15.1	2.9	12.1	0.5	0.0	0.9	20.9	18.7	3.1	4.4		5.4	6.3	
ZnO	144.7	78.9	34.9	106.2	134.6	62.5	162.9	64.9	104.8	95.2	143.8	96.7		78.9	77.8	
PbO	10.0	22.6	8.9	12.2	14.4	25.7	21.9	24.5	17.9	22.8	16.1	20.7		22.6	23.2	
La2O3	50.9	31.2	48.0	20.5	98.6	20.2	51.0	39.3	49.3	44.8	31.3	34.8		31.2	32.8	
CeO2	111.4	68.2	121.6	43.8	198.5	46.1	101.4	88.5	112.4	96.3	70.9	89.9		68.2	71.3	
ThO2	15.7	11.1	14.6	5.8	24.5	11.6	11.7	16.1	14.2	13.8	2.6	14.0		11.1	11.6	
Nd2O3	53.0	32.8	56.6	25.7	79.8	25.7	42.6	38.4	53.9	44.3	40.0	38.5		32.8	35.7	
U2O3	0.0	0.0	0.0	0.0	0.0	0.0	0.0	0.0	0.0	0.0	0.0	0.0		0.0	0.0	
Bi2O5	0.0	0.0	0.0	0.0	0.0	0.0	0.0	0.0	0.0	0.0	0.0	0.0		0.0	0.0	
Cs2O	0.0	0.0	0.0	0.0	0.0	0.0	0.0	0.0	0.0	0.0	0.0	0.0		0.0	0.0	
As2O5	0.0	0.0	0.0	0.0	0.0	0.0	0.0	0.0	0.0	0.0	0.0	0.0		0.0	0.0	
W2O3	0.0	0.0	0.0	0.0	0.0	0.0	0.0	0.0	0.0	0.0	0.0	0.0		0.0	0.0	
sum tr.	**1964**	**1686**	**2348**	**1497**	**3215**	**1325**	**3141**	**1891**	**2335**	**2128**	**2270**	**2103**		**1686**	**1692**	
in %	**0.20**	**0.17**	**0.23**	**0.15**	**0.32**	**0.13**	**0.31**	**0.19**	**0.23**	**0.21**	**0.23**	**0.21**		**0.17**	**0.17**	

	MUR 06 SMB07	MUR 06 SMB11	MUR 06 SMB12	MUR 06 SMB19	MUR 06 SMB20	MUR 06 SMB21	MUR 06 SMB22	MUR 06 SMB23	MUR 06 MP01		MUR 06 SMB22	MUR 06 SMB22R
Date	15-Jan-11	15-Jan-11	15-Jan-11	15-Jan-11	15-Jan-11	15-Jan-11	15-Jan-11	15-Jan-11	16-Jan-11		15-Jan-11	16-Jan-11
	Unnormalized Major Elements (Weight %):										**Unnormalized Major Elements (Weight %):**	
SiO2	72.13	70.69	71.95	71.10	69.53	67.80	67.40	65.90	67.73		67.40	67.47
TiO2	0.316	0.382	0.336	0.364	0.436	0.547	0.657	0.587	0.478		0.657	0.661
Al2O3	13.90	14.22	13.67	14.27	14.71	15.01	15.36	16.22	15.43		15.36	15.38
FeO*	2.18	2.37	2.39	2.34	2.91	3.52	4.27	3.74	2.97		4.27	4.25
MnO	0.061	0.051	0.063	0.057	0.068	0.075	0.097	0.082	0.067		0.097	0.097
MgO	0.70	0.74	0.67	0.76	0.80	1.06	1.23	1.16	1.51		1.23	1.24
CaO	1.16	1.53	1.26	1.57	1.43	1.62	2.12	2.06	2.49		2.12	2.12
Na2O	3.31	3.23	3.30	3.44	3.32	3.25	3.60	3.58	3.62		3.60	3.59
K2O	3.99	4.44	3.85	3.91	4.59	4.31	3.22	4.26	3.60		3.22	3.22
P2O5	0.172	0.136	0.143	0.142	0.141	0.160	0.181	0.203	0.194		0.181	0.182
Sum	97.92	97.79	97.64	97.95	97.93	97.36	98.13	97.79	98.09		98.13	98.21
	Normalized Major Elements (Weight %):										**Normalized Major Elements (Weight %):**	
SiO2	73.66	72.28	73.68	72.59	71.00	69.64	68.68	67.39	69.05		68.68	68.70
TiO2	0.322	0.390	0.344	0.372	0.445	0.562	0.670	0.601	0.487		0.670	0.673
Al2O3	14.20	14.54	14.00	14.57	15.02	15.42	15.65	16.59	15.73		15.65	15.66
FeO*	2.22	2.43	2.45	2.39	2.97	3.62	4.35	3.83	3.03		4.35	4.33
MnO	0.062	0.052	0.065	0.058	0.069	0.077	0.099	0.084	0.068		0.099	0.099
MgO	0.72	0.76	0.69	0.77	0.82	1.09	1.26	1.18	1.54		1.26	1.26
CaO	1.18	1.56	1.30	1.61	1.46	1.67	2.16	2.10	2.54		2.16	2.16
Na2O	3.38	3.30	3.38	3.51	3.39	3.34	3.67	3.66	3.69		3.67	3.66
K2O	4.07	4.54	3.95	3.99	4.69	4.43	3.28	4.36	3.67		3.28	3.28
P2O5	0.176	0.139	0.146	0.145	0.144	0.164	0.185	0.208	0.197		0.185	0.186
Total	100.00	100.00	100.00	100.00	100.00	100.00	100.00	100.00	100.00		100.00	100.00
	Unnormalized Trace Elements (ppm):										**Unnormalized Trace Elements (ppm):**	
Ni	0	4	2	3	4	4	7	6	10		7	8
Cr	13	15	12	14	16	20	22	20	35		22	23
Sc	6	6	7	6	8	10	11	11	9		11	11
V	24	30	25	26	31	40	48	49	42		48	51
Ba	321	569	322	532	511	558	467	660	430		467	467
Rb	202	163	187	155	186	177	183	184	184		183	184
Sr	108	147	105	158	134	175	161	191	162		161	162
Zr	115	142	133	139	159	206	248	204	137		248	246
Y	20	27	27	22	30	30	36	26	19		36	35
Nb	7.7	7.5	8.0	6.8	8.9	10.5	12.3	10.2	8.3		12.3	12.7
Ga	20	18	19	18	20	20	23	20	20		23	23
Cu	1	3	3	3	3	4	3	4	5		3	5
Zn	42	47	50	46	54	72	83	79	56		83	85
Pb	18	23	19	20	24	30	19	31	16		19	20
La	24	21	23	23	26	31	37	31	21		37	36
Ce	35	44	39	40	50	60	77	61	44		77	77
Th	10	11	11	10	12	12	14	12	11		14	14
Nd	19	25	24	21	25	31	36	34	24		36	36
Cs	8	6	10	7	10	4	14	11	12		14	15
sum tr.	991	1307	1023	1249	1311	1496	1503	1646	1246		1503	1510
in %	0.10	0.13	0.10	0.12	0.13	0.15	0.15	0.16	0.12		0.15	0.15
sum m+tr	98.01	97.92	97.75	98.07	98.06	97.51	98.28	97.96	98.22		98.28	98.37
M+Toxides	98.03	97.95	97.77	98.09	98.09	97.54	98.31	97.99	98.24		98.31	98.40
	Major elements are normalized on a volatile-free basis, with total Fe expressed as FeO.										**Major elements are normalized on a volatile**	
	"R" denotes a duplicate bead made from the same rock powder.										**"R" denotes a duplicate bead made from th**	
NiO	0.6	4.6	2.4	4.4	5.1	5.2	9.0	7.9	13.2		9.0	10.0
Cr2O3	19.0	21.9	17.1	19.7	23.1	29.5	32.4	29.7	50.9		32.4	33.2
Sc2O3	9.5	9.7	10.4	9.8	12.4	14.7	17.2	16.9	14.1		17.2	17.2
V2O3	34.7	43.4	36.2	38.5	45.5	59.0	71.2	72.1	62.2		71.2	74.9
BaO	357.9	635.3	359.4	594.4	570.1	623.5	521.9	737.1	480.4		521.9	521.7
Rb2O	220.7	178.0	204.3	169.3	203.4	193.6	200.1	201.3	201.6		200.1	201.1
SrO	127.2	173.5	123.9	187.1	158.9	207.4	190.8	225.6	191.6		190.8	191.0
ZrO2	156.5	194.0	181.7	189.1	216.4	281.8	338.6	278.5	186.6		338.6	335.6
Y2O3	25.5	34.0	33.9	27.3	38.4	38.4	46.1	33.5	24.4		46.1	44.7
Nb2O5	11.0	10.7	11.4	9.7	12.7	15.0	17.6	14.6	11.9		17.6	18.2
Ga2O3	26.3	24.7	25.8	24.2	26.6	26.3	31.1	27.4	26.6		31.1	30.8
CuO	1.8	3.1	3.3	3.9	3.4	5.5	3.5	4.9	6.6		3.5	6.3
ZnO	52.0	58.5	62.9	58.0	67.5	89.7	104.5	98.8	70.4		104.5	106.5
PbO	19.0	24.7	20.0	21.4	26.3	32.6	20.7	32.9	17.7		20.7	21.3
La2O3	27.8	24.5	26.7	26.4	30.6	36.5	43.7	36.7	24.9		43.7	42.3
CeO2	43.5	54.0	47.4	48.8	62.0	73.4	94.0	75.4	53.8		94.0	94.3
ThO2	10.5	11.9	12.5	11.1	12.7	13.6	15.0	13.5	11.6		15.0	15.8
Nd2O3	21.9	29.5	28.1	24.7	28.7	36.4	41.6	40.0	27.4		41.6	41.8
U2O3	0.0	0.0	0.0	0.0	0.0	0.0	0.0	0.0	0.0		0.0	0.0
Bi2O5	0.0	0.0	0.0	0.0	0.0	0.0	0.0	0.0	0.0		0.0	0.0
Cs2O	8.0	6.5	10.3	7.1	10.5	3.9	15.1	11.2	12.5		15.1	15.8
As2O5	0.0	0.0	0.0	0.0	0.0	0.0	0.0	0.0	0.0		0.0	0.0
W2O3	0.0	0.0	0.0	0.0	0.0	0.0	0.0	0.0	0.0		0.0	0.0
sum tr.	**1173**	**1543**	**1218**	**1475**	**1554**	**1786**	**1814**	**1958**	**1488**		**1814**	**1822**
in %	**0.12**	**0.15**	**0.12**	**0.15**	**0.16**	**0.18**	**0.18**	**0.20**	**0.15**		**0.18**	**0.18**